Journal of Mathematics in Industry
a SpringerOpen Journal

RESEARCH Open Access

Dual stochastic descriptions of streamflow dynamics under model ambiguity through a Markovian embedding

Hidekazu Yoshioka[1*] and Yumi Yoshioka[2]

*Correspondence: yoshih@jaist.ac.jp
[1] Japan Advanced Institute of Science and Technology, 1-1 Asahidai, Nomi, Ishikawa 923-1292, Japan
Full list of author information is available at the end of the article

Abstract

Hamilton–Jacobi–Bellman equation (HJBE) and backward stochastic differential equation (BSDE) are the two faces of stochastic control. We explore their equivalence focusing on a system of self-exciting and affine stochastic differential equations (SDEs) arising in streamflow dynamics. Our SDE is a finite-dimensional Markovian embedding of an infinite-dimensional jump-driven process called the superposition of continuous-state branching processes (a supCBI process). We formulate new ergodic control problems to evaluate the worst-case streamflow discharge in the long run and derive their HJBEs and ergodic BSDEs. The constant ambiguity aversion classically used in assessing model ambiguity must be modified in our case so that the optimality equations become well-posed. With a suitable modification of the ambiguity-aversion coefficient depending on the distributed reversion speed, we demonstrate that the solutions to the optimality equations are equivalent to each other in the sense that they lead to the same result. Finally, we apply the proposed framework to the computation of realistic cases with an existing record of discharge through a numerical Markovian embedding.

Keywords: Stochastic processes; Non-Markovian processes; Hamilton–Jacobi–Bellman equation; Backward stochastic differential equation; Numerical Markovian embedding; Streamflow management

1 Introduction

1.1 Problem background

Streamflow as a part of hydrological processes significantly affects not only the aquatic environments and ecosystems but also human living. On the one hand, streamflow regulation for hydropower generation can provide indispensable electricity for modern human life. On the other hand, it alternates downstream flow and temperature regimes, which negatively affect biological processes, such as fish migration [1, 2]. Extremely low flow due to water abstraction for human activities critically affects aquatic fauna as they may lack the adaptations to persist in such events [3]. Meanwhile, flood events cause damages, such as house collapses, wide inundations, and loss of human lives [4, 5]. Therefore, the modeling and control of streamflow dynamics have been a hotspot in research fields related to aquatic environments and ecosystems.

The stochastic modeling of streamflow dynamics has been a major approach toward their efficient analysis. Typically, a stochastic differential equation (SDE) is employed to describe the temporal evolution of Markovian state variables, such as the flow discharge [6, 7], water quality indices [8, 9], and river morphology [10], as well as key hydrological variables, such as active channel length [11]. Applied problems, such as flood diversion [12] and ecomorphodynamics [13], have also been analyzed using stochastic models.

Theories of optimal control and optimization covering dynamic programming [14] and martingale representation [15] have been established. Formally, dynamic programming and martingale representation are in a dual relationship as the two mutually different descriptions of the same control problem. In dynamic programming, the resolution of a control problem reduces to finding a classical or viscosity solution to a Hamilton–Jacobi–Bellman equation (HJBE) as a nonlinear degenerate parabolic partial differential equation [16]. Dynamic programming has often been used for detailed analysis of Markovian stochastic control problems with two to three state variables [17–19] as the computational costs of the modern numerical solver may become prohibitive in higher dimensions.

By contrast, in martingale representation, backward SDEs (BSDEs) have been used as the optimality equations, which are typically coupled with the forward SDEs of system dynamics. An advantage of using BSDEs is that they apply to non-Markovian, high-dimensional, and nearly optimal cases to which HJBEs do not apply [20–22]. However, the disadvantage is that BSDEs have many unknowns to be solved than HJBEs and the accuracy of their numerical solutions is often affected by statistical biases [23]. The rigorous equivalence of the two approaches has been proven under several regularity conditions [24]. Both HJBEs and BSDEs have been well-studied and compared in economics and related research fields. Nevertheless, to the best of our knowledge, their use for problems related to streamflow dynamics is still rare, despite their inherent stochasticity and the great demand for in-depth understanding and improvement of their management processes. This consideration motivates us to study HJBE and BSDE in the same streamflow optimization problem. Consistently analyzing their theories in a dual relationship would significantly deepen their mathematical structures and may yield secondary contributions to other aspects such as developing numerical methods for complex control problems in the future.

The stochastic control theory also contributes to evaluating model ambiguity. Indeed, a critical aspect in modeling with stochastic methods, such as SDEs, is that their identification in a real application contains some modeling errors (i.e., model ambiguity), resulting in biased analysis results and hence biased decisions. This ambiguity is due to the limited availability and quality of data and structural modeling assumptions [25, 26], which are difficult to avoid in most cases. A robust control approach [27] enabled us to describe model ambiguity as a control variable chosen by nature. Model ambiguity is evaluated in terms of the relative entropy between the baseline and worst-case models. With this approach, stochastic control under model ambiguity has successfully been studied in applied problems [28–31]. We employed this approach for environmental problems, such as managing riparian environments [32] and sediment replenishment [33]. However, the BSDE-based approach to these problems is still lacking, although several scholars have suggested that BSDEs with specific nonlinearities can handle model ambiguity [34–37].

1.2 Objectives and contributions

The objectives of this study are to formulate and analyze a kind of stochastic control model to evaluate streamflow dynamics under model ambiguity. We especially solve the same problem from the two different standpoints, HJBEs and BSDEs, and show their equivalence.

In the previous studies, we proposed a model that governs the discharge, the volume of water passing through a river cross-section in a unit time, as a jump-driven non-Markovian stochastic process having the subexponential autocorrelation function [38, 39]. The subexponential autocorrelation implies the existence of memory decaying slower than exponential speed in streamflow dynamics [40, 41], which should be considered in modeling and optimization for accurate prediction and management of aquatic environments. In this study, we extend the above model to an affine process model, called the superposition of continuous-state branching processes (supCBI process) [42, 43], having a more generic noise term accounting for clustered jump events, such as flood events, due to typhoons and rainy seasons. More specifically, the supCBI process is an analytically tractable model (i.e., its moments and autocorrelation are found analytically) that is able to represent jump-driven long-memory processes. It has widely been accepted in the pasthat the streamflow discharge reasonably follows a jump-driven SDE (e.g., [11]) (this is why we do not focus on processes without jumps), while they assume an exponential decay of the autocorrelation but real data of the discharge often exhibit a long memory as also reviewed in Yoshioka et al. [43]. In summary, the shortcoming of the other models is that they do not reproduce the long memory, while the advantage is that our model does without the critical loss of analytical tractability. In addition, the SDE representation harmonizes with the stochastic control, which is another advantage over the other models; however, especially the approaches based on long-run BSDEs have not been addressed in the literature including our works despite their relevance in analyzing the sustainable environmental management. To the best of our knowledge, HJBE and BSDE related to the supCBI process have not been studied yet.

The supCBI process is a tractable mathematical model as stated above. However, its optimization needs care because it is a non-Markovian process, as it is a superposition of infinitely many continuous-state branching (CBI) processes. We overcome this issue using the Markovian embedding [42–45] to rewrite or approximate a non-Markovian process to a system of Markovian processes. In the supCBI process, the superposition (i.e., integration) as the source of a subexponential decay is performed with respect to reversion speed distributed according to a probability measure. Then, we formulate a consistent finite-dimensional supCBI process as a system of affine processes by discretizing this probability measure. Our control problem is based on this finite-dimensional representation as presented in Fig. 1.

Our control problem is not a policy-making problem of some decision-maker but rather a worst-case dynamic optimization of long-run (i.e., time-average) discharge under model ambiguity in the sense of Anderson et al. [27]. This is an ergodic control problem of the finite-dimensional supCBI process subject to linear feedback so that the discharge is managed to be close to a target value by a water infrastructure. The problem is simple at a first glance but contains several nontrivial issues to be tackled. First, the conventional approach that penalizes model ambiguity with a constant ambiguity-aversion coefficient fails as the degree of the Markovian embedding becomes finer. Although similar well-posedness is-

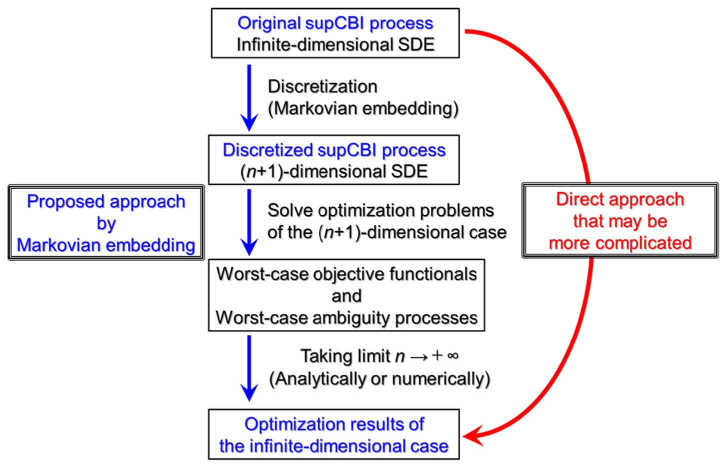

Figure 1 The approach used in this study

sues have been discussed in both finite- and infinite-dimensional diffusive SDEs with extreme ambiguity aversion [46], our problem varies in that it concerns jump-driven SDEs. We show that the ambiguity-aversion coefficient must depend on the distributed reversion speed to resolve this issue and present such an alternative with a correct scaling relationship between the ambiguity-aversion coefficient and reversion speed.

Another issue is that the research on the martingale representation-based approach to the ergodic control problem of jump-driven SDE is inadequate; only a few contributions have been made [47, 48]. Meanwhile, the dynamic programming of ergodic problems has been well-studied (e.g., Arapostathis et al. [49]). We show that, given an ambiguity-aversion coefficient, finding the worst-case upper and lower bounds of long-run discharge can be reduced to solving HJBEs, which have smooth solutions. Then, the aforementioned issue on the well-posedness related to the ambiguity-aversion coefficient is analyzed and a closed-form solution is obtained.

We also derive a BSDE, i.e., an ergodic BSDE (EBSDE), associated with our control problem. The difference between the present and existing EBSDEs is that the noise process in the former is the self-exciting jumps, while that in the latter is the Brownian motion [50, 51] or Lévy process [48]. BSDEs driven by self-exciting jumps have been introduced in pricing [52] and hedging and utility valuation [53]. Such BSDEs have also been used for dam operation but without considering model ambiguity [23]. To the best of our knowledge, EBSDE driven by self-exciting processes has neither been analyzed nor applied to engineering problems.

The worst-case upper and lower bounds of the long-run discharge for the original supCBI case are then obtained by a limit of the finite-dimensional case. Although we do not directly discuss the control in the infinite-dimensional case, it turns out that this limit exists and that it can be evaluated efficiently by numerical computation without resorting to a complex and time-consuming method such as Monte-Carlo methods. The tractability of our mathematical framework is attractive in this view.

Finally, we apply the proposed model to the evaluation of streamflow dynamics in a study site in Japan. This is based on a numerical implementation of the Markovian embedding whose convergence is demonstrated computationally. We also mention the applicability of the proposed model to the analysis of the dissolved silica (DSi) as a key driver of aquatic food webs and eutrophication [54–56]. In summary, we contribute to the theory, modeling, and application of the ergodic control problem of a non-Markovian process.

2 Mathematical model

2.1 supCBI process

The supCBI process and its finite-dimensional Markovian embedding are formulated. Hereinafter, time as a real parameter is expressed as t. The following is an overview of the model based on Yoshioka et al. [43]. We consider the temporal evolution of a discharge $X = (X_t)_{t\geq 0}$ at a cross-section of a river as a continuous-time scalar process. A CBI process with reversion speed $r > 0$ is a single-variable unique stationary càdlàg process $Y^{(r)} = (Y_t^{(r)})_{t\geq 0}$ governed by a self-exciting SDE [57]

$$\mathrm{d}Y_t^{(r)} = -rY_t^{(r)}\,\mathrm{d}t + \int_0^{+\infty}\int_0^{A+rBY_{t-}^{(r)}} zN_r(\mathrm{d}u,\mathrm{d}z,\mathrm{d}t), \quad t > 0 \tag{1}$$

given an initial condition $Y_0^{(r)} \geq 0$ (the left limit of the value of a stochastic process at time t is indicated with the subscript $t-$). A and B with $A^2 + B^2 > 0$ are non-negative parameters. N_r represents the Poisson random measure on $(0,+\infty)^3$; its compensated version $\tilde{N}_r$ is $\tilde{N}_r(\mathrm{d}u,\mathrm{d}z,\mathrm{d}s) = N_r(\mathrm{d}u,\mathrm{d}z,\mathrm{d}s) - \mathrm{d}u\nu(\mathrm{d}z)\,\mathrm{d}s$, with a Lévy measure $\nu(\mathrm{d}z)$ satisfying $\int_0^{+\infty}\min\{1,z\}\nu(\mathrm{d}z) < +\infty$ and $\int_{-\infty}^0 \nu(\mathrm{d}z) = 0$. The second term on the right-hand side of (1) is seen as a jump process having the state-dependent Lévy(-like) process with the corresponding jump measure $(A + rBY_{t-}^{(r)})\nu(\mathrm{d}z)$. The affine coefficient $A + rBY_{t-}^{(r)}$ represents the state-dependence of jumps, where the second term is scaled by r for later use.

We assume a tempered stable Lévy measure $\nu(\mathrm{d}z) = z^{-(\alpha+1)}\exp(-\beta z)\,\mathrm{d}z$ ($\alpha < 1$, $\beta > 0$) as a model for jumps with bounded variations [58]. Set $M_k = \int_0^{+\infty} z^k\nu(\mathrm{d}z)$ ($k = 1,2,3,\ldots$). This Lévy measure is the simplest one that can cover both finite ($\alpha < 0$) and infinite jump activities ($0 \leq \alpha < 1$). We assume

$$1 - BM_1 > 0, \tag{2}$$

which means that the self-exciting jumps are not large. The stationarity of the CBI process is broken without this condition [33].

Considering (1), the supCBI process $Y = (Y_t)_{t\geq 0}$ is formulated as the superposition (i.e., integration) of mutually independent CBI processes with respect to the reversion speed r [43]:

$$Y_t = Y_0 + \int_0^{+\infty} Y_t^{(r)}(\mathrm{d}r), \quad t \geq 0, \tag{3}$$

where $(Y_t^{(r)}(\mathrm{d}r))_{t\geq 0}$ ($r > 0$) is a measure-valued process governed by the formal SDE

$$\mathrm{d}Y_t^{(r)}(\mathrm{d}r) = -rY_t^{(r)}(\mathrm{d}r)\,\mathrm{d}t + \int_0^{A\pi(\mathrm{d}r)+rBY_{t-}^{(r)}(\mathrm{d}r)}\int_0^{\infty} z\mu_r(\mathrm{d}u,\mathrm{d}z,\mathrm{d}t). \tag{4}$$

Each μ_r ($r > 0$) is formally a mutually independent Poisson random measure for a different r having the compensator $\mathrm{d}u \times \nu(\mathrm{d}z) \times \mathrm{d}t$, and π is a probability density on $(0,+\infty)$

satisfying the usual normalization condition $\int_0^{+\infty} \pi(\mathrm{d}r) = 1$, having the average, and the regularity condition

$$\int_0^{+\infty} \frac{1}{r} \pi(\mathrm{d}r) < +\infty. \tag{5}$$

The condition (5) implies that if $\pi(\mathrm{d}r)$ has a probability density function, it behaves near $r = 0$ as $r^{\alpha'}$ ($\alpha' > 0$). Notably, the superposition can be understood via Lévy basis (e.g., [59]), but we do not directly use this property. Instead, we consider a discretized process as explained later in this subsection.

Remark 1 Equation (4) is formal as it is a measure-valued SDE. Rigorously, the process Y has been considered as a limit in the sense of characteristic functions, namely, in the sense of law, of the finite-dimensional process Y_n explained later (Appendix A of Yoshioka [42]).

Condition (5) is necessary to have statistical moments of Y at a stationary state [42, 60]. Under (5), the stationary statistics are [42]

$$\mathbb{E}[Y_t] = \frac{AM_1}{1 - BM_1} \int_0^{+\infty} \frac{1}{r} \pi(\mathrm{d}r), \tag{6}$$

$$\mathbb{E}\left[\left(Y_t - \mathbb{E}[Y_t]\right)^2\right] = \frac{AM_2}{2(1 - BM_1)^2} \int_0^{+\infty} \frac{1}{r} \pi(\mathrm{d}r), \tag{7}$$

$$\begin{aligned} \mathrm{Cor}(s) &= \frac{\mathbb{E}[(Y_{t+s} - \mathbb{E}[Y_{t+s}])(Y_t - \mathbb{E}[Y_t])]}{\mathbb{E}[(Y_t - \mathbb{E}[Y_t])^2]} \\ &= \left[\int_0^{+\infty} \frac{1}{r} \pi(\mathrm{d}r)\right]^{-1} \int_0^{+\infty} \frac{1}{r} \exp\left(-r(1 - BM_1)s\right) \pi(\mathrm{d}r), \quad s \geq 0. \end{aligned} \tag{8}$$

Higher statistical moments, such as skewness and kurtosis, can also be obtained.

We present a Markovian embedding of the supCBI process (3). The key of the embedding is the representation (3) itself, where the right-hand side is seen as an informal sum (actually, an integration) of mutually independent supCBI processes. This type of formulation is also the foundation of the other superpositions of stochastic processes, such as the superposition of Ornstein–Uhlenbeck processes [59].

For $n \in \mathbb{N}$, $n \geq 2$, set the discrete probability measure π_n as $\pi_n(\mathrm{d}r) = \sum_{i=1}^n \delta_{r_i} c_i$, where δ_r is the Dirac's delta at $r > 0$, and the non-negative sequences $\{r_i\}_{i=1,2,\ldots,n}$ and $\{c_i\}_{i=1,2,\ldots,n}$ are given using another sequence $\{\eta_i\}_{i=1,2,\ldots,n}$ with $0 = \eta_0 < \eta_1 < \cdots < \eta_{n-1} < \eta_n = +\infty$ as

$$c_i = \int_{\eta_{i-1}}^{\eta_i} \pi(\mathrm{d}r) \quad \text{and} \quad r_i = \frac{1}{c_i} \int_{\eta_{i-1}}^{\eta_i} r\pi(\mathrm{d}r) \quad (1 \leq i \leq n). \tag{9}$$

We also set a discrete measure $l_n(\mathrm{d}r) = \sum_{i=1}^n \delta_{r_i}$. In addition, for a fixed $n \in \mathbb{N}$, we can find a continuous function $c : [0, +\infty) \to [0, +\infty)$, such that $c(r_i) = c_i$ $(1 \leq i \leq n)$ with an abuse of notations.

The Markovian embedding is discretizing the integral in the right-hand side as a finite sum to obtain the finite-dimensional supCBI process $Y_n = (Y_{n,t})_{t \geq 0}$ as

$$Y_{n,t} = \sum_{i=1}^n Y_t^{(r_i)} = \int_0^{+\infty} Y_t^{(r)} l_n(\mathrm{d}r), \quad t \geq 0 \tag{10}$$

with CBI processes

$$\mathrm{d}Y_t^{(r)} = -rY_t^{(r)}\,\mathrm{d}t + \int_0^{+\infty}\int_0^{c(r)A+rBY_{t-}^{(r)}} zN_r(\mathrm{d}u,\mathrm{d}z,\mathrm{d}t), \quad t>0 \tag{11}$$

defined at each $r = r_i$ ($1 \le i \le n$) with an initial condition. This is a natural discrete analogue of (4). The choice of $\{\eta_i\}_{i=1,2,\dots,n}$ is not arbitrary and should be specified so that Y_n converges to Y in the sense of law [42, 43]. The convergence in this sense is satisfied in the discretization scheme employed in Sect. 5.3. The measure-based representation, such as (10) turns out to be useful in finding linkages between the original and discretized supCBI processes. In addition, it allows us to analyze them with the least coexistence of summations and integrals. For the finite-dimensional supCBI process, a natural filtration generated by $\{N_{r_i}\}_{i=1,2,\dots,n}$ is denoted as $\mathcal{F} = (\mathcal{F}_t)_{t\ge 0}$, which is augmented by sets of measure zero as usual. Hereinafter, $\mathcal{F}$-measurable and $\mathcal{F}$-adapted processes are called measurable and adapted processes without reference to $\mathcal{F}$.

We end this subsection by presenting the discharge $X = (X_t)_{t\ge 0}$ subject to a linear feedback control. In the previous studies, the discharge was not controlled, where we used $X_t = \underline{X} + Y_t$ with a constant $\underline{X} \ge 0$ representing the minimum discharge [38, 42]. We extend this by incorporating linear feedback as [43]

$$X_t = \underline{X} + \omega\int_0^t e^{-\rho(t-s)}X_s\,\mathrm{d}s + Y_{n,t}, \quad t\ge 0, \tag{12}$$

where $\rho > 0$ and $\omega \in \mathbb{R}$ are parameters of the feedback control, $\omega > 0$ and $\omega < 0$ represents the water addition and abstraction, respectively. This is the simplest model to control the discharge based on the observable inflow information (the last term of (12)) and the past duration (the second term of (12)). The problem without any control is obtained by setting $\omega = 0$, suggesting that the proposed model generalizes the evaluation problem of the supCBI process.

As we want to consider an ergodic control problem where the discharge eventually becomes stationary, we need the condition $\rho > \omega$. Indeed, a straightforward calculation yields

$$\mathbb{E}[X_t] = \frac{\rho}{\rho-\omega}\left(\underline{X} + \mathbb{E}[Y_{n,t}]\right) \quad \text{with } \mathbb{E}[Y_{n,t}] = \frac{AM_1}{1-BM_1}\int_0^{+\infty}\frac{1}{r}\pi_n(\mathrm{d}r). \tag{13}$$

From (13), if the feedback is imposed so that the discharge X_t is close to a prescribed target $\hat{X} > 0$, we should choose (ρ,ω) so that

$$\mathbb{E}[X_t] = \hat{X} \quad \text{or equivalently} \quad \omega = \rho\left(1 - \frac{\underline{X} + \mathbb{E}[Y_{n,t}]}{\hat{X}}\right). \tag{14}$$

We also present the differential form of (12):

$$\begin{aligned}\mathrm{d}X_t = {} & \left\{-(\rho-\omega)X_t + \rho\underline{X} + \int_0^{+\infty}(\rho - r)Y_t^{(r)} l_n(\mathrm{d}r)\right\}\mathrm{d}t \\ & + \int_0^{+\infty}\int_0^{+\infty}\int_0^{c(r)A+rBY_{t-}^{(r)}} zN_r(\mathrm{d}u,\mathrm{d}z,\mathrm{d}t) l_n(\mathrm{d}r), \quad t>0\end{aligned} \tag{15}$$

with $X_0 = \underline{X} + Y_{n,0}$.

Remark 2 The discharge for the original supCBI process can be analogously defined by simply omitting the subscript n in the discussion above. This formal relationship between the original and finite-dimensional supCBI processes is exploited in the sequel. See, also Remark 4 on the notion of symbols.

Remark 3 What is essential in our model, especially from the well-posedness of the ambiguity aversion that we will discuss, is the superposition of the measure-valued functions rather than the feedback term. In fact, qualitatively, the same result holds if we use the feedback $\int_0^t \omega(\rho - X_s)\,\mathrm{d}s$ with $\omega, \rho > 0$. Our results therefore apply to the case without feedback regulations.

2.2 Ambiguity model

Ambiguity is formulated as a distortion of the Poisson random measure N_r such that its compensator $\mathrm{d}u\nu(\mathrm{d}z)\,\mathrm{d}s$ is modulated by some measurable and càdlàg field $\phi(\cdot) = (\phi_t(\cdot,\cdot))_{t\geq 0}$ with $\phi_t : (0,+\infty)^2 \to (0,+\infty)$, called the ambiguity process, as $\mathrm{d}u\phi_t(r,z)\nu(\mathrm{d}z)\,\mathrm{d}s$ [27]. This modulation is performed under a measure change based on the Radon–Nikodym derivative as in Yoshioka and Tsujimura [33] with a suitable modification to account for the distributed reversion speed.

The benchmark probability measure is denoted as $\mathbb{P}$ under which the compensator of N_r is $\mathrm{d}u\nu(\mathrm{d}z)\,\mathrm{d}s$. Hereinafter, the expectation under a probability measure $\mathbb{Q}$ is expressed as $\mathbb{E}_{\mathbb{Q}}[\cdot]$. The Poisson random measure N_r is denoted as $N_{\mathbb{Q},r}$ under $\mathbb{Q}$. We introduce the exponential process $\mathfrak{M} = (\mathfrak{M}_t)_{t\geq 0}$ depending on ϕ as follows:

$$\mathfrak{M}_t = \exp\left\{\int_0^{+\infty} m_t(r) l_n(\mathrm{d}r)\right\}, \quad t \geq 0 \tag{16}$$

with

$$m_t(r) = \int_0^t \int_0^{+\infty} \int_0^{c(r)A+rBY_{s-}^{(r)}} \begin{pmatrix} \ln\phi_{s-}(z)\{N_{\mathbb{P},r}(\mathrm{d}u,\mathrm{d}z,\mathrm{d}s) - \mathrm{d}u\nu(\mathrm{d}z)\,\mathrm{d}s\} \\ -(\phi_s(z) - 1 - \ln\phi_s(z))\,\mathrm{d}u\nu(\mathrm{d}z)\,\mathrm{d}s \end{pmatrix}. \tag{17}$$

The dependence of ϕ on r is suppressed in (17) to simplify the descriptions, which are used in the sequel.

For ϕ, we assume the following conditions under which (16) is a positive martingale [61]:

$$\begin{aligned} &\mathbb{E}_{\mathbb{P}}\left[\int_0^{+\infty}\int_0^t \int_0^{+\infty}\int_0^{c(r)A+rBY_{s-}^{(r)}} \left(\phi_s(z) - 1 - \ln\phi_s(z)\right)\mathrm{d}u\nu(\mathrm{d}z)\,\mathrm{d}s l_n(\mathrm{d}r)\right] \\ &\quad < +\infty, \quad t > 0 \end{aligned} \tag{18}$$

and

$$\begin{aligned} &\mathbb{E}_{\mathbb{P}}\left[\exp\left\{\int_0^{+\infty}\int_0^t \int_0^{+\infty}\int_0^{c(r)A+rBY_{s-}^{(r)}} \left(1 - \phi_s(z) + \phi_s(z)\ln\phi_s(z)\right)\mathrm{d}u\nu(\mathrm{d}z)\,\mathrm{d}s l_n(\mathrm{d}r)\right\}\right] \\ &\quad < +\infty, \quad t > 0. \end{aligned} \tag{19}$$

As $\mathfrak{M}$ is a positive martingale with $\mathfrak{M}_0 = 1$, it is a Radon–Nikodym derivative that can be written as $\frac{\mathrm{d}\mathbb{Q}(\phi)}{\mathrm{d}\mathbb{P}}$ between $\mathbb{P}$ and $\mathbb{Q}(\phi)$ such that the compensator of the Poisson random measure $N_{\mathbb{Q}(\phi),r}$ on $\mathbb{Q}(\phi)$ is $\mathrm{d}u\phi_t(z)\nu(\mathrm{d}z)\,\mathrm{d}s$. We say that there is an ambiguity unless $\phi_t(\cdot)\equiv 1$ $(t\geq 0)$. The ambiguity level is measured by the relative entropy [27]

$$\begin{aligned}
&\mathbb{E}_{\mathbb{P}}\left[\frac{\mathrm{d}\mathbb{Q}(\phi)}{\mathrm{d}\mathbb{P}}|_t \ln \frac{\mathrm{d}\mathbb{Q}(\phi)}{\mathrm{d}\mathbb{P}}|_t\right] \\
&\quad = \mathbb{E}_{\mathbb{Q}(\phi)}\left[\ln \frac{\mathrm{d}\mathbb{Q}(\phi)}{\mathrm{d}\mathbb{P}}|_t\right] \\
&\quad = \mathbb{E}_{\mathbb{Q}(\phi)}\left[\int_0^{+\infty} m_t(r) l_n(\mathrm{d}r)\right] \\
&\quad = \mathbb{E}_{\mathbb{Q}(\phi)}\left[\int_0^{+\infty}\int_0^t\int_0^{+\infty}\int_0^{c(r)A+rBY_{s-}^{(r)}}\begin{pmatrix}\ln\phi_{s-}(z)(N_{\mathbb{Q}(\phi),r}(\mathrm{d}u,\mathrm{d}z,\mathrm{d}s) \\ -\,\mathrm{d}u\nu(\mathrm{d}z)\,\mathrm{d}s) \\ -\,(\phi_s(z)-1-\ln\phi_s(z))\,\mathrm{d}u\nu(\mathrm{d}z)\,\mathrm{d}s\end{pmatrix} l_n(\mathrm{d}r)\right] \\
&\quad = \mathbb{E}_{\mathbb{Q}(\phi)} \\
&\qquad \left[\int_0^{+\infty}\int_0^t\int_0^{+\infty}\int_0^{c(r)A+rBY_{s-}^{(r)}}\begin{pmatrix}\ln\phi_{s-}(z)(N_{\mathbb{Q}(\phi),r}(\mathrm{d}u,\mathrm{d}z,\mathrm{d}s) \\ -\,\mathrm{d}u\phi_s(z)\nu(\mathrm{d}z)\,\mathrm{d}s) \\ +\,(\phi_s(z)\ln\phi_s(z) \\ -\,\phi_s(z)+1)\,\mathrm{d}u\nu(\mathrm{d}z)\,\mathrm{d}s\end{pmatrix} l_n(\mathrm{d}r)\right] \\
&\quad = \mathbb{E}_{\mathbb{Q}(\phi)}\left[\int_0^{+\infty}\int_0^t \left(c(r)A + rBY_s^{(r)}\right)\right. \\
&\qquad \times \left.\int_0^{+\infty}\left(\phi_s(z)\ln\phi_s(z)-\phi_s(z)+1\right)\nu(\mathrm{d}z)\,\mathrm{d}s l_n(\mathrm{d}r)\right], \quad t\geq 0.
\end{aligned} \tag{20}$$

We end this subsection by defining the admissible set $\mathcal{A}$ of ambiguity processes ϕ:

$$\mathcal{A} = \left\{\phi = \left(\phi_t(\cdot)\right)_{t\geq 0} | \phi \text{ is adapted and measurable, and satisfies (18) and (19).}\right\}. \tag{21}$$

Hereinafter, we only consider ambiguity processes ϕ belonging to $\mathcal{A}$. The reference to $\mathcal{A}$ is omitted when there will be no confusion.

Remark 4 The mapping ϕ may depend on $n\in\mathbb{N}$ to define the measure π_n, but its dependence on n is suppressed in what follows. The same rule applies to the mappings b and κ appearing in the sections below. Sometimes, we write a short description such that $b(r_i)$ is described as b_i for simplicity. This notation will be useful to better understand the finite- and infinite-dimensional problems.

2.3 Worst-case evaluation problems

We introduce the worst-case maximization and minimization problems to evaluate the maximum and minimum long-run discharge under the ambiguity. We explain the maximization case in this study; the minimization case can be handled similarly through a suitable change of the sign of the ambiguity-aversion coefficient.

Set the penalty $\mathbb{A}(t,\phi)$ of the ambiguity given ϕ as

$$\begin{aligned}
\mathbb{A}(t,\phi) = \mathbb{E}_{\mathbb{Q}(\phi)}&\left[\int_0^{+\infty}\frac{1}{\psi(r)}\int_0^t \left(c(r)A + rBY_s^{(r)}\right)\right. \\
&\times\left.\int_0^{+\infty}\left(\phi_s(z)\ln\phi_s(z)-\phi_s(z)+1\right)\nu(\mathrm{d}z)\,\mathrm{d}s l_n(\mathrm{d}r)\right], \quad t\geq 0
\end{aligned} \tag{22}$$

with an ambiguity-aversion coefficient $\psi(\cdot)$ as a positive univariate function. This ψ represents the degree of ambiguity aversion of the decision-maker who evaluates the discharge in a manner that small ψ (resp., large ψ) represents small (resp., large) penalization of the ambiguity in our problem.

The penalty $\mathbb{A}$ reduces to the usual relative entropy when ψ is a constant, which corresponds to the penalization used in the classical control problems [27], whereas it is rather a weighted version of the relative entropy with respect to the reversion speed $r > 0$. This case is understood as a situation where the decision-maker has a distributed ambiguity aversion against the different time scales in the discharge timeseries.

Then, the worst-case evaluation problem of the long-run discharge is formulated as follows:

$$\text{Find } \sup_{\phi\in\mathcal{A}} \limsup_{T\to+\infty} \left(\frac{1}{T}\mathbb{E}_{\mathbb{Q}(\phi)}\left[\int_0^T X_s \,\mathrm{d}s\right] - \frac{1}{T}\mathbb{A}(T,\phi) \right). \tag{23}$$

The supremum (23), if it exists, is denoted as H. The maximizing ϕ, if it exists, is denoted as ϕ^* and is called the worst-case ambiguity. The goal of this control problem is to find H, ϕ^*, and each term of (23) given ϕ^*. Indeed, what is important would be not the optimized objective (23) itself but the worst-case discharge (first term) having the physical meaning and the corresponding relative entropy (second term).

For later use, we provide the expectations of $\mathbb{E}_{\mathbb{Q}(\phi)}[Y_t^{(r_i)}]$ ($i = 1,2,\ldots,n$) and $\mathbb{E}_{\mathbb{Q}(\phi)}[X_t]$ given $\phi_t \equiv e^{\theta z}$ ($\theta < \beta$) such that $\bar{M}_1 = \int_0^{+\infty} e^{\theta z} z v(\mathrm{d}z) < B^{-1}$. Such a θ exists by (2). Taking the expectations of (11) and (15) yields

$$\frac{\mathrm{d}}{\mathrm{d}t}\mathbb{E}_{\mathbb{Q}(\phi)}\left[Y_t^{(r_i)}\right] = c_i A\bar{M}_1 - r_i(1 - B\bar{M}_1)\mathbb{E}_{\mathbb{Q}(\phi)}\left[Y_t^{(r_i)}\right], \quad t > 0 \tag{24}$$

and

$$\begin{aligned}\frac{\mathrm{d}}{\mathrm{d}t}\mathbb{E}_{\mathbb{Q}(\phi)}[X_t] = \Bigg\{ & -(\rho-\omega)\mathbb{E}_{\mathbb{Q}(\phi)}[X_t] + \rho\underline{X} + A\bar{M}_1 \\ & + \sum_{i=1}^n \big(\rho - r_i(1 - B\bar{M}_1)\big)\mathbb{E}_{\mathbb{Q}(\phi)}\left[Y_t^{(r_i)}\right] \Bigg\}, \quad t > 0.\end{aligned} \tag{25}$$

Therefore, we obtain the following proposition.

Proposition 1 *Assume $\phi_t \equiv e^{\theta z}$ ($\theta < \beta$) such that $\bar{M}_1 = \int_0^{+\infty} e^{\theta z} z v(\mathrm{d}z) < B^{-1}$. Then, it follows that*

$$\left|\mathbb{E}_{\mathbb{Q}(\phi)}\left[Y_T^{(r_i)}\right]\right|, \left|\mathbb{E}_{\mathbb{Q}(\phi)}[X_T]\right| \le C_0 + C_1\exp(-C_2 T), \quad T \ge 0, i = 1,2,\ldots,n \tag{26}$$

with some positive constants C_0, C_1, C_2 independent of T. In addition, for any real bounded sequence $\{a_i\}_{i=0,1,\ldots,n}$, it follows that

$$\lim_{T\to+\infty} \frac{1}{T}\mathbb{E}_{\mathbb{Q}(\phi)}\left[a_0 X_T + \sum_{i=1}^n a_i Y_T^{(r_i)}\right] = 0. \tag{27}$$

Proof of Proposition 1 The first statement (26) is realized by a straightforward calculation by $\rho > \omega$ and the assumption on θ. The second statement (27) is a consequence of the first one (26). Indeed, we have

$$
\begin{aligned}
&\lim_{T\to+\infty} \frac{1}{T}\mathbb{E}_{\mathbb{Q}(\phi)}\left[a_0 X_T + \sum_{i=1}^{n} a_i Y_T^{(r_i)}\right] \\
&= a_0 \lim_{T\to+\infty} \frac{1}{T}\mathbb{E}_{\mathbb{Q}(\phi)}[X_T] + \lim_{T\to+\infty} \frac{1}{T}\sum_{i=1}^{n} a_i \mathbb{E}_{\mathbb{Q}(\phi)}\left[Y_T^{(r_i)}\right] \\
&\le |a_0| \lim_{T\to+\infty} \frac{1}{T}\left|\mathbb{E}_{\mathbb{Q}(\phi)}[X_T]\right| + \sum_{i=1}^{n} |a_i| \lim_{T\to+\infty} \frac{1}{T}\left|\mathbb{E}_{\mathbb{Q}(\phi)}\left[Y_T^{(r_i)}\right]\right| \\
&\le |a_0| \frac{1}{T}(C_0 + C_1) + \sum_{i=1}^{n} |a_i| \lim_{T\to+\infty} \frac{1}{T}(C_0 + C_1) \\
&= 0.
\end{aligned}
\tag{28}
$$

The other side of the inequality can be obtained similarly. □

Remark 5 The minimizing problem can be formulated as follows:

$$
\text{Find } \inf_{\phi\in\mathcal{A}} \liminf_{T\to+\infty}\left(\frac{1}{T}\mathbb{E}_{\mathbb{Q}(\phi)}\left[\int_0^T X_s\,\mathrm{d}s\right] + \frac{1}{T}\mathbb{A}(T,\phi)\right). \tag{29}
$$

In the HJBE and EBSDE presented later, H and ϕ^* in the minimization case are obtained in a similar way.

3 HJBE formulation

3.1 Derivation

Following the ergodic control formulation (e.g., [9, 33]), the HJBE associated with (29) is

$$
\begin{aligned}
&-h + x + \left\{-(\rho-\omega)x + \rho\underline{X} + \sum_{i=1}^{n}(\rho - r_i)y_i\right\}\frac{\partial V}{\partial x} - \sum_{i=1}^{n} r_i y_i \frac{\partial V}{\partial y_i} \\
&\quad + \sup_{\{\phi_i\}=1,2,\dots,n}\left\{\sum_{i=1}^{n}(c_i A + r_i B y_i)\right. \\
&\quad \times \left.\int_0^\infty \left(\Delta V_i(z_i)\phi_i(z) - \frac{1}{\psi(r_i)}\bigl(\phi_i(z)\ln\phi_i(z) - \phi_i(z) + 1\bigr)\right)\nu(\mathrm{d}z_i)\right\} = 0
\end{aligned}
\tag{30}
$$

with

$$
\begin{aligned}
\Delta V_i(z_i) = {}& V(x + z_i, y_0, y_1, \dots, y_i + z_i, \dots, y_n) \\
& - V(x, y_0, y_1, \dots, y_i, \dots, y_n), \quad 1 \le i \le n
\end{aligned}
\tag{31}
$$

whose solution is a couple (h, V) of a constant $h \in \mathbb{R}$ and a smooth function $V = V(x, y_0, y_1, \dots, y_n) \in C^1(\mathbb{R}^{n+1})$ satisfying the linear growth condition with a constant $C > 0$:

$$
\limsup_{|x|,|y_1|,|y_2|,\dots,|y_n|\to+\infty} \frac{V(x, y_0, y_1, \dots, y_n)}{1 + |x| + \sum_{i=1}^{n}|y_i|} \le C. \tag{32}
$$

This HJBE (30) is rewritten by calculating the "sup" term as follows:

$$\begin{aligned} &-h + x + \left\{-(\rho - \omega)x + \rho \underline{X} + \sum_{i=1}^{n} (\rho - r_i) y_i \right\} \frac{\partial V}{\partial x} - \sum_{i=1}^{n} r_i y_i \frac{\partial V}{\partial y_i} \\ &\quad + \sum_{i=1}^{n} (c_i A + r_i B y_i) \int_0^{\infty} \frac{1}{\psi(r_i)} \bigl(\exp\bigl(\psi(r_i) \Delta V_i(z_i)\bigr) - 1\bigr) \nu(\mathrm{d}z_i) = 0. \end{aligned} \tag{33}$$

Based on the Markovian control ansatz (e.g., [14]), we guess that the maximizer of (23) is obtained through V as follows:

$$\begin{aligned} \phi_t^* &\equiv \bigl\{\phi_i^*\bigl(z, X_t, Y_t^{(r_i)}, \dots, Y_t^{(r_n)}\bigr)\bigr\}_{i=1,2,\dots,n} \\ &= \underset{\phi = \{\phi_i\}=1,2,\dots,n}{\arg\max} \left\{ \sum_{i=1}^{n} \int_0^{\infty} \left(\Delta V_i(z_i) \phi_i(z) - \frac{1}{\psi(r_i)} \bigl(\phi_i(z) \ln \phi_i(z) - \phi_i(z) + 1\bigr) \right) \nu(\mathrm{d}z_i) \right\} \\ &= \bigl\{\exp\bigl(\psi(r_i) \Delta V_i(z_i)\bigr)\bigr\}_{i=1,2,\dots,n}, \end{aligned} \tag{34}$$

where the last line is evaluated at $(X_t, Y_t^{(r_i)}, \dots, Y_t^{(r_n)})$.

3.2 Solution and optimality

We explicitly solve the HJBE (33) and justify (34) under an assumption of the ambiguity-aversion coefficient ψ. The solution obtained below has a simple form, while its existence is nontrivial.

Proposition 2 *The HJBE admits a solution (h, V) of the affine form*

$$V(x, y_1, \dots, y_n) = c + ax + \sum_{i=1}^{n} (b_i - a) y_i, \tag{35}$$

$$h = \rho a \underline{X} + A \sum_{i=1}^{n} \frac{c_i}{\psi(r_i)} \int_0^{\infty} \bigl(\exp\bigl(\psi(r_i) b_i z_i\bigr) - 1\bigr) \nu(\mathrm{d}z_i) \tag{36}$$

if each element of $\{\psi(r_i)\}_{i=1,2,\dots,n}$ and B are sufficiently small, where $c \in \mathbb{R}$ is an arbitrary constant, $a = \frac{1}{\rho - \omega} > 0$, and $b_i > 0$ $(1 \le i \le n)$, represented by some function $b(\cdot)$ as $b_i = b(r_i)$, is a unique positive solution in $(0, \frac{\beta}{\psi(r_i)})$ of

$$b = F_i(b) \equiv \frac{\rho a}{r_i} + \frac{B}{\psi(r_i)} \int_0^{\infty} \bigl(\exp\bigl(\psi(r_i) b z_i\bigr) - 1\bigr) \nu(\mathrm{d}z_i), \quad 1 \le i \le n. \tag{37}$$

Proof of Proposition 2 The representation (35) and (36) are obtained by substituting (35) into (33). Specifically, we obtain

$$\begin{aligned} &-h + x + \left\{-(\rho - \omega)x + \rho \underline{X} + \sum_{i=1}^{n} (\rho - r_i) y_i \right\} a - \sum_{i=1}^{n} r_i y_i (b_i - a) \\ &\quad + \sum_{i=1}^{n} (c_i A + r_i B y_i) \int_0^{\infty} \frac{1}{\psi(r_i)} \bigl(\exp\bigl(\psi(r_i) b_i z_i\bigr) - 1\bigr) \nu(\mathrm{d}z_i) = 0 \end{aligned} \tag{38}$$

by $\Delta V_i(z_i) = az + (b_i - a)z = b_i z$, $1 \le i \le n$. Comparing each coefficient multiplied by $x, y_1, \ldots, y_n$ yields (35)–(37).

What remains to be proven is the statement that there exists a small $\{\psi(r_i)\}_{i=1,2,\ldots,n}$ such that (37) admits a unique positive solution. Fix $i \in \{1,2,\ldots,n\}$, we have

$$F_i(0) = \frac{\rho a}{r_i} > 0, \tag{39}$$

$$\begin{aligned} \frac{\mathrm{d}F_i(b)}{\mathrm{d}b} &= B\int_0^\infty z_i \exp\bigl(\psi(r_i)b_i z_i\bigr)\nu(\mathrm{d}z_i) > 0, \\ \frac{\mathrm{d}F_i(0)}{\mathrm{d}b} &= B\int_0^\infty z_i \nu(\mathrm{d}z_i) = BM_1 \in (0,1), \end{aligned} \tag{40}$$

$$\frac{\mathrm{d}^2F_i(b)}{\mathrm{d}b^2} = B\psi(r_i)\int_0^\infty z_i^2 \exp\bigl(\psi(r_i)b_i z_i\bigr)\nu(\mathrm{d}z_i) > 0. \tag{41}$$

Therefore, $F_i(\cdot)$ is strictly increasing and convex. By the classical intermediate value theorem and (39), owing to assuming a tempered stable type ν, (37) admits a unique solution in $(0, \frac{\beta}{\psi(r_i)})$ if

$$F_i\left(\frac{\beta}{\psi(r_i)}\right) < \frac{\beta}{\psi(r_i)}, \tag{42}$$

or equivalently if

$$\begin{aligned} \frac{\rho a}{r_i}\psi(r_i) + B\int_0^\infty \bigl(\exp(\beta z_i) - 1\bigr)\nu(\mathrm{d}z_i) &= \frac{\rho a}{r_i}\psi(r_i) + B\bigl(-\Gamma(-\alpha)\bigr)\beta^\alpha \\ &= \frac{\rho a}{r_i}\psi(r_i) + B\beta^{\alpha-1}\Gamma(1-\alpha)\beta\frac{-\Gamma(-\alpha)}{\Gamma(1-\alpha)} \\ &= \frac{\rho a}{r_i}\psi(r_i) + \frac{\beta}{\alpha}BM_1 \\ &< \beta, \end{aligned} \tag{43}$$

namely, if

$$\frac{\rho a}{r_i}\psi(r_i) + \frac{\beta}{\alpha}BM_1 < \beta \tag{44}$$

with the Gamma function $\Gamma(\cdot)$, which is possible if we choose a sufficiently small $\psi(r_i) > 0$ for all i and $B > 0$. The proof is completed because the equation to find b_i is decoupled with each other. □

As a byproduct of *Proof of Proposition* 2, we understand how the parameter dependence of ψ plays a role. The inequality (44) implies that in the constant case $\psi(\cdot) \equiv \bar{\psi}$ common in the classical ambiguity model [27], it is impossible to choose a small $\bar{\psi}$ uniformly with respect to n, namely, uniformly with respect to the degree of Markovian embedding. This is because the term $\frac{\rho a}{r_1}$ diverges to $+\infty$ as n increases for generic π. The coefficient ψ must be parameter-dependent such that $\frac{\rho a}{r_i}\psi(r_i) < +\infty$ independent of n. The reasonable choice is

$$\psi(r) \equiv \bar{\psi} r \tag{45}$$

with a constant $\bar{\psi} > 0$. In this case, (43) reduces to

$$\rho a\bar{\psi} + B\int_0^{\infty}\big(\exp(\beta z) - 1\big)\nu(\mathrm{d}z) < \beta, \tag{46}$$

which is satisfied independent of n if $B, \bar{\psi} > 0$ are small. The present choice (45) means that the ambiguity aversion is stronger for a larger reversion speed r corresponding to the high-frequency components of the discharge. In the other words, the ambiguity aversion against small reversion speed r (i.e., base flow) that would critically affect the long-term dynamics should not be critically large as the state dynamics become unbounded. Notably, any other monomial scaling cannot yield an r-independent condition (46), suggesting that the correct scaling is essential for our problem.

From Proposition 2 and (34), we guess the worst-case ambiguity

$$\phi_i^*\big(z, X_t, Y_t^{(r_1)}, \dots, Y_t^{(r_n)}\big) = \exp\big(\psi(r_i)b_i z_i\big). \tag{47}$$

The next proposition shows that this ϕ^* is indeed optimal.

Proposition 3 *Under the assumption of Proposition* 2 *with* (45), *there are sufficiently small* B *and* $\bar{\psi}$ *independent of* n *such that the admissibility conditions* (18) *and* (19) *are satisfied by* (47). *In addition,* ϕ^* *is the worst-case ambiguity and* $h = H$.

Proof of Proposition 3 The first statement is already proven above. The main tasks of the proof are the verification of the admissibility by a direct substitution and the verification of the optimality by exploiting the smoothness of the guessed solution.

We need to check that this ϕ^* satisfies both (18) and (19). This is done as follows. For (18), with $\phi = \phi^*$, we have

$$\begin{aligned}
&\mathbb{E}_{\mathbb{P}}\left[\int_0^{+\infty}\int_0^t\int_0^{+\infty}\int_0^{c(r)A + rBY_s^{(r)}}\big(\phi_t^*(z) - 1 - \ln\phi_t^*(z)\big)\,\mathrm{d}u\,\nu(\mathrm{d}z)\,\mathrm{d}s\,l_n(\mathrm{d}r)\right]\\
&\quad= \mathbb{E}_{\mathbb{P}}\left[\int_0^{+\infty}\int_0^{+\infty}\big(\exp\big(\psi(r_i)b(r_i)z\big) - 1 - \psi(r_i)b(r_i)z\big)\nu(\mathrm{d}z)\right.\\
&\qquad\left.\times\int_0^t\big(c(r)A + rBY_s^{(r)}\big)\,\mathrm{d}s\,l_n(\mathrm{d}r)\right]\\
&\quad= \sum_{i=1}^n\int_0^{+\infty}\big(\exp\big(\psi(r_i)b(r_i)z\big) - 1 - \psi(r_i)b(r_i)z\big)\nu(\mathrm{d}z)\\
&\qquad\times\mathbb{E}_{\mathbb{P}}\left[\int_0^t\big(c_iA + r_iBY_s^{(r_i)}\big)\,\mathrm{d}s\right],\quad t > 0.
\end{aligned}\tag{48}$$

For $i = 1, 2, \dots, n$, we obtain the existence of the integral

$$\begin{aligned}
&\int_0^{+\infty}\big(\exp\big(\psi(r_i)b_iz\big) - 1 - \psi(r_i)b_iz\big)\nu(\mathrm{d}z)\\
&\quad= \int_0^{+\infty}\big(\exp\big(\psi(r_i)b_iz\big) - 1\big)\nu(\mathrm{d}z) - M_1\psi(r_i)b_i.
\end{aligned}\tag{49}$$

We also have the estimate

$$\begin{aligned}
&\mathbb{E}_{\mathbb{P}}\left[\int_0^t \left(c_i A + r_i B Y_s^{(r_i)}\right) \mathrm{d}s\right] \\
&= c_i A t + r_i B \mathbb{E}_{\mathbb{P}}\left[\int_0^t Y_s^{(r_i)} \,\mathrm{d}s\right] \\
&= c_i A t + r_i B \int_0^t \mathbb{E}_{\mathbb{P}}\left[Y_s^{(r_i)}\right] \mathrm{d}s < +\infty, \quad t > 0.
\end{aligned} \tag{50}$$

Because of $b_i \in (0, \frac{\beta}{\psi(r_i)})$, $\int_0^\infty z \exp(\psi(r_i) b_i z)\nu(\mathrm{d}z) < +\infty$; hence, (50) follows. Consequently, (18) is satisfied by the mutual independence of each $Y^{(r_i)}$ with the specified $\phi = \phi^*$.

For (19), we have

$$\begin{aligned}
&\mathbb{E}_{\mathbb{P}}\left[\exp\left\{\int_0^{+\infty}\int_0^t\int_0^{+\infty}\int_0^{c(r)A + rBY_s^{(r)}} \left(1 - \phi_s(z) + \phi_s(z)\ln\phi_s(z)\right) \mathrm{d}u\nu(\mathrm{d}z)\,\mathrm{d}s l_n(\mathrm{d}r)\right\}\right] \\
&= \mathbb{E}_{\mathbb{P}}\left[\exp\left\{\sum_{i=1}^n \begin{pmatrix} \int_0^{+\infty}(1 - \exp(\psi(r_i)b_i z) \\ + \psi(r_i)b_i z \exp(\psi(r_i)b_i z))\nu(\mathrm{d}z) \\ \times \int_0^t (c_i A + r_i B Y_s^{(r_i)})\,\mathrm{d}s \end{pmatrix}\right\}\right], \quad t > 0.
\end{aligned} \tag{51}$$

As in the previous case, we have

$$\int_0^{+\infty} \left(1 - \exp\left(\psi(r_i)b_i z\right) + \psi(r_i)b_i z \exp\left(\psi(r_i)b_i z\right)\right)\nu(\mathrm{d}z) \le C \tag{52}$$

with a constant $C > 0$ independent of i, n. So, (51) yields

$$\begin{aligned}
&\mathbb{E}_{\mathbb{P}}\left[\exp\left\{\int_0^{+\infty}\int_0^t\int_0^{+\infty}\int_0^{c(r)A + rBY_s^{(r)}} \left(1 - \phi_s(z) + \phi_s(z)\ln\phi_s(z)\right) \mathrm{d}u\nu(\mathrm{d}z)\,\mathrm{d}s l_n(\mathrm{d}r)\right\}\right] \\
&\le \mathbb{E}_{\mathbb{P}}\left[\exp\left\{C\sum_{i=1}^n \int_0^t \left(c_i A + r_i B Y_s^{(r_i)}\right) \mathrm{d}s\right\}\right] \\
&= \prod_{i=1}^n \mathbb{E}_{\mathbb{P}}\left[\exp\left\{C\int_0^t \left(c_i A + r_i B Y_s^{(r_i)}\right) \mathrm{d}s\right\}\right] \\
&= \prod_{i=1}^n \mathbb{E}_{\mathbb{P}}\left[\exp\left\{c_i C A t + r_i C B\int_0^t Y_s^{(r_i)} \,\mathrm{d}s\right\}\right] \\
&= \exp(CAt)\prod_{i=1}^n \mathbb{E}_{\mathbb{P}}\left[\exp\left(r_i C B\int_0^t Y_s^{(r_i)} \,\mathrm{d}s\right)\right], \quad t > 0.
\end{aligned} \tag{53}$$

Here, we again used the mutual independence of each $Y^{(r_i)}$. We must show the existence of each expectation at the bottom of (53). However, this is possible with a small B (Appendix of Yoshioka and Tsujimura [33]). Consequently, both (18) and (19) are satisfied by the guessed control.

Once the admissibility of ϕ^* is obtained, it remains to prove $h = H$. As ϕ^* is independent of the state variables, the optimality, namely, h equals the maximum value of (23) follows.

Below, we exploit the affine functional form of V in (35). More specifically, we have

$$\begin{aligned}
&\sum_{i=1}^{n}\sum_{0<\tau_{i,j}<T}\Big(V\big(X_{\tau_{i,j}-}+\Delta N_{i,j},\big\{\delta_{i,k}\big(Y^{(r_i)}_{\tau_{k,j}-}+\Delta N_{k,j}\big)\big\}_{k=1,2,\dots,n}\big)\\
&\qquad - V\big(X_{\tau_{i,j}-},\big\{\delta_{i,k}Y^{(r_i)}_{\tau_{k,j}-}\big\}_{k=1,2,\dots,n}\big)\Big)\\
&\quad=\sum_{i=1}^{n}\sum_{0<\tau_{i,j}<T}\big(a(X_{\tau_{i,j}-}+\Delta N_{i,j})+(b_i-a)\big(Y^{(r_i)}_{\tau_{i,j}-}+\Delta N_{i,j}\big)-aX_{\tau_{i,j}-}-(b_i-a)Y^{(r_i)}_{\tau_{i,j}-}\big)\\
&\quad=\sum_{i=1}^{n}\sum_{0<\tau_{i,j}<T}b_i\Delta N_{i,j},
\end{aligned}\tag{54}$$

where $\delta_{\cdot,\cdot}$ is the Kronecker's delta, $\{\tau_{i,j}\}_{j=1,2,3,\dots}$ is an increasing sequence representing the jth jump of N_{r_i} and the summation $\sum_{0<\tau_{i,j}<T}$ is with respect to all j satisfying $0<\tau_{i,j}<T$, and $\Delta N_{i,j}$ is the jump of N_{r_i} at $\tau_{i,j}$. Because each N_{r_i} has a bounded variation and hence $\sum_{0<\tau_{i,j}<T}\Delta N_{i,j}$ is bounded a.s. and its compensator is $\int_0^T(c_iA+r_iBY_s^{(r_i)})\int_0^\infty\phi_{i,s}(z)\nu(\mathrm{d}z_i)\,\mathrm{d}s$, the expectation of this summation under $\mathbb{E}_{\mathbb{Q}(\phi)}$ is given by

$$\begin{aligned}
&\mathbb{E}_{\mathbb{Q}(\phi)}\left[\sum_{i=1}^{n}\sum_{0<\tau_{i,j}<T}b_i\Delta N_{i,j}\right]\\
&\quad=\mathbb{E}_{\mathbb{Q}(\phi)}\left[\sum_{i=1}^{n}b_i\sum_{0<\tau_{i,j}<T}\Delta N_{i,j}\right]\\
&\quad=\sum_{i=1}^{n}b_i\mathbb{E}_{\mathbb{Q}(\phi)}\left[\sum_{0<\tau_{i,j}<T}\Delta N_{i,j}\right]\\
&\quad=\sum_{i=1}^{n}b_i\mathbb{E}_{\mathbb{Q}(\phi)}\left[\int_0^T\big(c_iA+r_iBY_s^{(r_i)}\big)\int_0^\infty\phi_{i,s}(z)\nu(\mathrm{d}z_i)\,\mathrm{d}s\right]\\
&\quad=\mathbb{E}_{\mathbb{Q}(\phi)}\left[\sum_{i=1}^{n}\int_0^T\big(c_iA+r_iBY_s^{(r_i)}\big)\int_0^\infty b_i\phi_{i,s}(z)\nu(\mathrm{d}z_i)\,\mathrm{d}s\right]\\
&\quad=\mathbb{E}_{\mathbb{Q}(\phi)}\left[\sum_{i=1}^{n}\int_0^T\big(c_iA+r_iBY_s^{(r_i)}\big)\int_0^\infty\Delta V_i(z_i)\phi_{i,s}(z)\nu(\mathrm{d}z_i)\,\mathrm{d}s\right].
\end{aligned}\tag{55}$$

By Dynkin's formula and (30) with any solution (h,V) in Proposition 2, we have (integrands are evaluated at $(X_s,\{Y_s^{(r_i)}\}_{i=1,2,\dots,n})$)

$$\begin{aligned}
&\mathbb{E}_{\mathbb{Q}(\phi)}\big[V\big(X_T,\big\{Y_T^{(r_i)}\big\}_{i=1,2,\dots,n}\big)\big]-V\big(x,\{y_i\}_{i=1,2,\dots,n}\big)\\
&\quad=\mathbb{E}_{\mathbb{Q}(\phi)}\left[\int_0^T\begin{pmatrix}\{-(\rho-\omega)X_s+\rho\underline{X}+\sum_{i=1}^n(\rho-r_i)Y_s^{(r_i)}\}\frac{\partial V}{\partial x}-\sum_{i=1}^n r_iY_s^{(r_i)}\frac{\partial V}{\partial y_i}\\ +\sum_{i=1}^n(c_iA+r_iBY_s^{(r_i)})\int_0^\infty\Delta V_i(z_i)\phi_{i,s}(z)\nu(\mathrm{d}z_i)\end{pmatrix}\mathrm{d}s\right]\\
&\quad=Th-\mathbb{E}_{\mathbb{Q}(\phi)}\left[\int_0^T X_s\,\mathrm{d}s\right]
\end{aligned}$$

$$+\mathbb{E}_{\mathbb{Q}(\phi)}\left[\int_0^T\begin{pmatrix}\sum_{i=1}^n(c_iA+r_iBY_s^{(r_i)})\int_0^\infty\Delta V_i(z_i)\phi_{i,s}(z)\nu(\mathrm{d}z_i)\\ -\sup_{\{\phi_i\}_{=1,2,\ldots,n}}\{\sum_{i=1}^n(c_iA+r_iBY_s^{(r_i)})\\ \times\int_0^\infty\Big(\begin{smallmatrix}\Delta V_i(z_i)\phi_{i,s}(z)\\ -\frac{1}{\psi(r_i)}(\phi_{i,s}(z)\ln\phi_{i,s}(z)-\phi_{i,s}(z)+1)\end{smallmatrix}\Big)\nu(\mathrm{d}z_i)\}\end{pmatrix}\mathrm{d}s\right], \tag{56}$$

for $T>0$, from which we obtain

$$\begin{aligned}h={}&\frac{\mathbb{E}_{\mathbb{Q}(\phi)}[V(X_T,\{Y_T^{(r_i)}\}_{i=1,2,\ldots,n})]-V(x,\{y\}_{i=1,2,\ldots,n})}{T}+\frac{1}{T}\mathbb{E}_{\mathbb{Q}(\phi)}\left[\int_0^T X_s\,\mathrm{d}s\right]\\&+\frac{1}{T}\mathbb{E}_{\mathbb{Q}(\phi)}\left[\int_0^T\begin{pmatrix}-\sum_{i=1}^n(c_iA+r_iBY_s^{(r_i)})\int_0^\infty\Delta V_i(z_i)\phi_{i,s}(z)\nu(\mathrm{d}z_i)\\ +\sup_{\{\phi_i\}_{=1,2,\ldots,n}}\{\sum_{i=1}^n(c_iA+r_iBY_s^{(r_i)})\\ \times\int_0^\infty\Big(\begin{smallmatrix}\Delta V_i(z_i)\phi_{i,s}(z)\\ -\frac{1}{\psi(r_i)}(\phi_{i,s}(z)\ln\phi_{i,s}(z)-\phi_{i,s}(z)+1)\end{smallmatrix}\Big)\nu(\mathrm{d}z_i)\}\end{pmatrix}\mathrm{d}s\right].\end{aligned} \tag{57}$$

Because $\phi\in\mathcal{A}$ is arbitrary, the linear growth condition (32), and **Proposition 1**, we obtain

$$\begin{aligned}h&\geq\limsup_{T\to+\infty}\frac{1}{T}\left\{\begin{matrix}\mathbb{E}_{\mathbb{Q}(\phi)}[\int_0^T X_s\,\mathrm{d}s]\\ -\mathbb{E}_{\mathbb{Q}(\phi)}[\int_0^T\sum_{i=1}^n(c_iA+r_iBY_s^{(r_i)})\\ \times\int_0^\infty\frac{1}{\psi(r_i)}(\phi_{i,s}(z)\ln\phi_{i,s}(z)-\phi_{i,s}(z)+1)\nu(\mathrm{d}z_i)\,\mathrm{d}s]\end{matrix}\right\}\\&=\limsup_{T\to+\infty}\frac{1}{T}\left\{\mathbb{E}_{\mathbb{Q}(\phi)}\left[\int_0^T X_s\,\mathrm{d}s\right]-\mathbb{A}(T,\phi)\right\}.\end{aligned} \tag{58}$$

Hence, we obtain $h\geq H$ and the equality $h=H$ follows with $\phi=\phi^*$ of (47), proving the optimality. □

Remark 6 If (ρ,ω) satisfies (14), H depends on them only through $\rho a=\frac{\rho}{\rho-\omega}=$ constant.

4 EBSDE formulation

4.1 Derivation

We provide another view of the control problem (23) from the perspective of EBSDE. The key relationship is the duality between the HJBE and EBSDE [47, 50], which is used here as well. We will use the finite-dimensional supCBI process. In this subsection, we heuristically derive the EBSDE. Its optimality is verified in the next subsection.

EBSDE characterizes the problem differently from HJBE as it depends on a Martingale representation of auxiliary stochastic processes. Our BSDE is categorized as an EBSDE whose solution involves some adapted processes and a real constant. This constant is expected to be identified as the maximized objective H. Given an admissible ϕ, set the BSDE whose solution is the triplet (W,U,η): an adapted square-integrable scalar process $W=(W_t)_{t\geq0}$, a predictable process $U(\cdot,\cdot)=(U_t(\cdot,\cdot))_{t\geq0}$, such that

$$\begin{aligned}&\mathbb{E}_{\mathbb{Q}(\phi)}\left[\int_0^{+\infty}\int_t^T\int_0^{+\infty}\int_0^{c(r)A+rBY_{s-}^{(r)}}\{U_s(r,z)\}^2\phi_s(z)\,\mathrm{d}u\nu(\mathrm{d}z)\,\mathrm{d}sl_n(\mathrm{d}r)\right]\\&<+\infty,\quad 0\leq t\leq T\end{aligned} \tag{59}$$

and a constant $\eta\in\mathbb{R}$:

$$-\mathrm{d}W_t=\big(\Psi(X_t,Y_t,U_t)-\eta\big)\,\mathrm{d}t$$

$$
\begin{aligned}
&- \int_0^{+\infty}\int_0^{+\infty}\int_0^{c(r)A+rBY_{t-}^{(r)}} U_t(r,z)\big(N_{\mathbb{P},r}(\mathrm{d}u,\mathrm{d}z,\mathrm{d}t) \\
&- \mathrm{d}u\nu(\mathrm{d}z)\,\mathrm{d}t\big)l_n(\mathrm{d}r)\ (\text{Under}\mathbb{P}) \\
={}& \bigg(\Psi(X_t,Y_t,U_t) - \eta \\
&- \int_0^{+\infty}\big(c(r)A + rBY_t^{(r)}\big)\int_0^{+\infty} U_t(r,z)\big(\phi_t(z)-1\big)\nu(\mathrm{d}z)l_n(\mathrm{d}r)\bigg)\,\mathrm{d}t \\
&- \int_0^{+\infty}\int_0^{+\infty}\int_0^{c(r)A+rBY_{t-}^{(r)}} U_t(r,z)\big(N_{\mathbb{Q}(\phi),r}(\mathrm{d}u,\mathrm{d}z,\mathrm{d}t) - \mathrm{d}u\phi_t(z)\nu(\mathrm{d}z)\,\mathrm{d}t\big) \\
&\times l_n(\mathrm{d}r)\ \big(\text{Under}\mathbb{Q}(\phi)\big), \quad t>0,
\end{aligned} \tag{60}
$$

$\Psi(X_t,Y_t,U_t) = \Psi(X_t,\{Y_t^{(r_i)}\}_{1\le i\le n},\{U_t^{(r_i)}\}_{1\le i\le n})$ with some $\Psi:\mathbb{R}^{2n+1}\to\mathbb{R}$ determined later. From (60), we obtain

$$
\begin{aligned}
W_0 - W_T = -T\eta + \int_0^T \bigg(&\Psi(X_t,Y_t,U_t) - \int_0^{+\infty}\big(c(r)A + rBY_t^{(r)}\big)\int_0^{+\infty} U_t(r,z)\big(\phi_t(z)-1\big) \\
&\times \nu(\mathrm{d}z)l_n(\mathrm{d}r)\bigg)\,\mathrm{d}t \\
&- \int_0^{+\infty}\int_0^T\int_0^{+\infty}\int_0^{c(r)A+rBY_{t-}^{(r)}} U_t(r,z)\big(N_{\mathbb{Q}(\phi),r}(\mathrm{d}u,\mathrm{d}z,\mathrm{d}t) \\
&- \mathrm{d}u\phi_t(z)\nu(\mathrm{d}z)\,\mathrm{d}t\big)l_n(\mathrm{d}r).
\end{aligned} \tag{61}
$$

Then, we deduce

$$
\begin{aligned}
\eta ={}& \frac{1}{T}\mathbb{E}_{\mathbb{Q}(\phi)}[W_T - W_0] \\
&+ \frac{1}{T}\mathbb{E}_{\mathbb{Q}(\phi)}\bigg[\int_0^T \bigg(\Psi(X_t,Y_t,U_t) \\
&- \int_0^{+\infty}\big(c(r)A + rBY_t^{(r)}\big)\int_0^{+\infty} U_t(r,z)\big(\phi_t(z)-1\big)\nu(\mathrm{d}z)l_n(\mathrm{d}r)\bigg)\,\mathrm{d}t\bigg] \\
={}& \frac{1}{T}\mathbb{E}_{\mathbb{Q}(\phi)}[W_T - W_0] \\
&+ \frac{1}{T}\mathbb{E}_{\mathbb{Q}(\phi)}\left[\int_0^T \begin{pmatrix} \Psi(X_t,Y_t,U_t) \\ -\int_0^{+\infty}(c(r)A + rBY_t^{(r)})\int_0^{+\infty} U_t(r,z)(\phi_t(z)-1)\nu(\mathrm{d}z)l_n(\mathrm{d}r) \\ -L(X_t,Y_t,\phi_t)\end{pmatrix}\mathrm{d}t\right] \\
&+ \frac{1}{T}\mathbb{E}_{\mathbb{Q}(\phi)}\bigg[\int_0^T L(X_t,Y_t,\phi_t)\,\mathrm{d}t\bigg]
\end{aligned} \tag{62}
$$

with the choices

$$
\begin{aligned}
L(X_t,Y_t,\phi_t) = X_t - \int_0^{\infty}&\big(c(r)A + rBY_t^{(r)}\big)\frac{1}{\psi(r)} \\
&\times \int_0^{+\infty}\big(\phi_t(z)\ln\phi_t(z) - \phi_t(z) + 1\big)\nu(\mathrm{d}z)l_n(\mathrm{d}r)
\end{aligned} \tag{63}
$$

and

$$\Psi(X_t,Y_t,U_t) = \sup_{\phi_t(\cdot)>0}\left\{\int_0^{+\infty}\left(c(r)A + rBY_t^{(r)}\right)\right.$$
$$\left.\times\int_0^{+\infty}U_t(r,z)\left(\phi_t(z)-1\right)\nu(\mathrm{d}z)l_n(\mathrm{d}r) + L(X_t,Y_t,\phi_t)\right\}. \tag{64}$$

With these L and Ψ, we may expect the representation

$$H = \sup_{\phi\in\mathcal{A}}\limsup_{T\to+\infty}\frac{1}{T}\mathbb{E}_{\mathbb{Q}(\phi)}\left[\int_0^T L(X_t,Y_t,U_t,\phi_t)\,\mathrm{d}t\right]. \tag{65}$$

If

$$\limsup_{T\to+\infty}\frac{1}{T}\mathbb{E}_{\mathbb{Q}(\phi)}[W_T - W_0] = 0, \tag{66}$$

we obtain the inequality

$$\begin{aligned}
\eta &= \limsup_{T\to+\infty}\frac{1}{T}\left(\begin{matrix}\mathbb{E}_{\mathbb{Q}(\phi)}\left[\int_0^T\left(\begin{matrix}\Psi(X_t,Y_t,U_t)\\ -\int_0^{+\infty}(c(r)A+rBY_t^{(r)})\int_0^{+\infty}U_t(r,z)(\phi_t(z)-1)\nu(\mathrm{d}z)l_n(\mathrm{d}r)\\ -L(X_t,Y_t,\phi_t)\end{matrix}\right)\mathrm{d}t\right]\\ +\,\mathbb{E}_{\mathbb{Q}(\phi)}[\int_0^T L(X_t,Y_t,\phi_t)\,\mathrm{d}t]\end{matrix}\right)\\
&\geq \limsup_{T\to+\infty}\frac{1}{T}\left(\begin{matrix}\mathbb{E}_{\mathbb{Q}(\phi)}[\int_0^T(\Psi(X_t,Y_t,U_t)-\Psi(X_t,Y_t,U_t))\,\mathrm{d}t]\\ +\,\mathbb{E}_{\mathbb{Q}(\phi)}[\int_0^T L(X_t,Y_t,\phi_t)\,\mathrm{d}t]\end{matrix}\right)\\
&= \limsup_{T\to+\infty}\frac{1}{T}\mathbb{E}_{\mathbb{Q}(\phi)}\left[\int_0^T L(X_t,Y_t,\phi_t)\,\mathrm{d}t\right]
\end{aligned} \tag{67}$$

and hence

$$\eta \geq \sup_{\phi\in\mathcal{A}}\limsup_{T\to+\infty}\frac{1}{T}\mathbb{E}_{\mathbb{Q}(\phi)}\left[\int_0^T L(X_t,Y_t,U_t,\phi_t)\,\mathrm{d}t\right] = H. \tag{68}$$

The right-hand side of (64) is rewritten as

$$\begin{aligned}
&\sup_{\phi_t(\cdot)>0}\left\{\begin{matrix}\int_0^{+\infty}\left(c(r)A+rBY_t^{(r)}\right)\int_0^{+\infty}U_t(r,z)\left(\phi_t(z)-1\right)\nu(\mathrm{d}z)l_n(\mathrm{d}r)\\ +\,X_t - \left(c(r)A+rBY_t^{(r)}\right)\int_0^{\infty}\frac{1}{\psi(r)}\int_0^{+\infty}\left(\phi_t(z)\ln\phi_t(z)-\phi_t(z)+1\right)\nu(\mathrm{d}z)l_n(\mathrm{d}r)\end{matrix}\right\}\\
&\quad= X_t + \left(c(r)A+rBY_t^{(r)}\right)\int_0^{+\infty}\int_0^{+\infty}\sup_{\phi_t(\cdot)>0}\left(U_t(r,z)\left(\phi_t(z)-1\right)\right.\\
&\qquad\left.-\frac{\phi_t(z)\ln\phi_t(z)-\phi_t(z)+1}{\psi(r)}\right)\nu(\mathrm{d}z)l_n(\mathrm{d}r),
\end{aligned} \tag{69}$$

for which we have

$$\begin{aligned}
&\sup_{\phi_t(\cdot)>0}\left(U_t(r,z)\left(\phi_t(z)-1\right)-\frac{\phi_t(z)\ln\phi_t(z)-\phi_t(z)+1}{\psi(r)}\right)\\
&\quad= U_t(r,z)\left(e^{\psi(r)U_t(r,z)}-1\right)-\frac{\psi(r)U_t(r,z)e^{\psi(r)U_t(r,z)}-e^{\psi(r)U_t(r,z)}+1}{\psi(r)}\\
&\quad= \frac{e^{\psi(r)U_t(r,z)}-\psi(r)U_t(r,z)-1}{\psi(r)}
\end{aligned} \tag{70}$$

with the maximizer of the "sup" term given by $\phi_t = \tilde{\phi}_t = e^{\psi(r)U_t(r,z)}$. Consequently, we obtain the equality

$$\eta = \frac{1}{T}\mathbb{E}_{\mathbb{Q}(\tilde{\phi})}\left[\int_0^T L(X_t, Y_t, U_t, \tilde{\phi}_t)\,\mathrm{d}t\right] \geq H \tag{71}$$

and hence $\eta = H$ and $\tilde{\phi} = \phi^*$ by (68) if this $\phi = \tilde{\phi}$ is admissible.

From (64) and (69), our EBSDE on $\mathbb{P}$ should have the form

$$\begin{aligned}
-\mathrm{d}W_t &= \bigl(\Psi(X_t, Y_t, U_t) - \eta\bigr)\,\mathrm{d}t \\
&\quad - \int_0^{+\infty}\int_0^{+\infty}\int_0^{c(r)A + rBY_{t-}^{(r)}} U_t(r,z) \\
&\quad \times \bigl(N_{\mathbb{P},r}(\mathrm{d}u, \mathrm{d}z, \mathrm{d}t) - \mathrm{d}u\nu(\mathrm{d}z)\,\mathrm{d}t\bigr)l_n(\mathrm{d}r), \quad t > 0
\end{aligned} \tag{72}$$

with Ψ given by

$$\begin{aligned}
\Psi(X_t, Y_t, U_t) = X_t &+ \int_0^{+\infty}\bigl(c(r)A + rBY_t^{(r)}\bigr) \\
&\times \int_0^{+\infty}\frac{e^{\psi(r)U_t(r,z)} - \psi(r)U_t(r,z) - 1}{\psi(r)}\nu(\mathrm{d}z)l_n(\mathrm{d}r).
\end{aligned} \tag{73}$$

4.2 Optimality

We verify the optimality of the EBSDE (73) using a guessed-solution technique. We guess the affine form

$$\begin{aligned}
&W_t = pX_t + \int_0^{+\infty}\bigl(\varphi(r) - p\bigr)Y_t^{(r)}l_n(\mathrm{d}r) \quad \text{and} \\
&U_t(r_i, z) = \kappa(r_i)z \quad (i = 1, 2, \ldots, n), t > 0
\end{aligned} \tag{74}$$

with some constant p and fields $\varphi(\cdot)$, $\kappa(\cdot)$. A straightforward calculation shows

$$\begin{aligned}
-\mathrm{d}W_t &= -p\,\mathrm{d}X_t - \int_0^{+\infty}\varphi(r)\,\mathrm{d}Y_t^{(r)}l_n(\mathrm{d}r) \\
&= -p\left\{-(\rho - \omega)X_t + \rho\underline{X} + \int_0^{+\infty}(\rho - r)Y_t^{(r)}l_n(\mathrm{d}r)\right\}\mathrm{d}t \\
&\quad - p\int_0^{+\infty}\int_0^{+\infty}\int_0^{c(r)A + rBY_{t-}^{(r)}} zN_{\mathbb{P},r}(\mathrm{d}u, \mathrm{d}z, \mathrm{d}t)l_n(\mathrm{d}r) \\
&\quad - \left\{-\int_0^{+\infty}\bigl(\varphi(r) - p\bigr)rY_t^{(r)}l_n(\mathrm{d}r)\,\mathrm{d}t\right. \\
&\quad \left. + \int_0^{+\infty}\bigl(\varphi(r) - p\bigr)\int_0^{+\infty}\int_0^{c(r)A + r_iBY_{t-}^{(r)}} zN_{\mathbb{P},r}(\mathrm{d}u, \mathrm{d}z, \mathrm{d}t)l_n(\mathrm{d}r)\right\} \\
&= \left\{p(\rho - \omega)X_t - p\rho\underline{X} + \int_0^{+\infty}\bigl\{\varphi(r)r - p\rho\bigr\}Y_t^{(r)}l_n(\mathrm{d}r)\right\}\mathrm{d}t \\
&\quad - \int_0^{+\infty}\varphi(r)\int_0^{+\infty}\int_0^{c(r)A + r_iBY_{t-}^{(r)}} zN_{\mathbb{P},r}(\mathrm{d}u, \mathrm{d}z, \mathrm{d}t)l_n(\mathrm{d}r).
\end{aligned} \tag{75}$$

Substituting (74) and (75) into (72) yields

$$\begin{aligned}
&\left\{p(\rho-\omega)X_t - p\rho\underline{X} + \int_0^{+\infty}\{\varphi(r)r - p\rho\}Y_t^{(r)} l_n(\mathrm{d}r)(\mathrm{d}r)\right\}\mathrm{d}t \\
&\quad - \int_0^{+\infty}\varphi(r)\int_0^{+\infty}\int_0^{c(r)A + r_i B Y_{t-}^{(r)}} z N_{\mathbb{P},r}(\mathrm{d}u,\mathrm{d}z,\mathrm{d}t)\pi(\mathrm{d}r) \\
&= \left(X_t + \int_0^{+\infty}\left(c(r)A + rBY_t^{(r)}\right)\int_0^{+\infty}\frac{e^{\psi(r)\kappa(r)z}-1}{\psi(r)}\nu(\mathrm{d}z) l_n(\mathrm{d}r) - \eta\right)\mathrm{d}t \\
&\quad - \int_0^{+\infty}\int_0^{+\infty}\int_0^{c(r)A + rBY_{t-}^{(r)}} \kappa(r) z N_{\mathbb{P},r}(\mathrm{d}u,\mathrm{d}z,\mathrm{d}t) l_n(\mathrm{d}r).
\end{aligned} \tag{76}$$

From this identity, we obtain

$$p(\rho-\omega) = 1 \quad \text{or equivalently} \quad p = \frac{1}{\rho-\omega}, \tag{77}$$

$$\int_0^{+\infty}\left\{\varphi(r)r - p\rho - rB\int_0^{+\infty}\frac{e^{\psi(r)\kappa(r)z}-1}{\psi(r)}\nu(\mathrm{d}z)\right\}Y_t^{(r)} l_n(\mathrm{d}r) = 0, \tag{78}$$

$$\int_0^{+\infty}\left(\varphi(r) - \kappa(r)\right) l_n(\mathrm{d}r) = 0, \tag{79}$$

and

$$\begin{aligned}
\eta &= p\rho\underline{X} + A\int_0^{+\infty} c(r)\int_0^{+\infty}\frac{e^{\psi(r)\kappa(r)z}-1}{\psi(r)}\nu(\mathrm{d}z) l_n(\mathrm{d}r) \\
&= p\rho\underline{X} + A\int_0^{+\infty}\int_0^{+\infty}\frac{e^{\psi(r)\kappa(r)z}-1}{\psi(r)}\nu(\mathrm{d}z)\pi_n(\mathrm{d}r).
\end{aligned} \tag{80}$$

Considering the discreteness of the measure $\pi_n(\mathrm{d}r)$, from (79), we obtain $\varphi = \kappa$ a.e. on π_n. Then, from (78), we have

$$\varphi(r) = \frac{p\rho}{r} + B\int_0^{+\infty}\frac{e^{\psi(r)\varphi(r)z}-1}{\psi(r)}\nu(\mathrm{d}z) \quad \text{a.e. on } \pi_n. \tag{81}$$

From Proposition 2, we find the equivalence

$$p = a, \qquad \varphi(r_i) = \kappa(r_i) = b_i \quad (1 \le i \le n), \quad \text{and} \quad \eta = h = H. \tag{82}$$

As we already know $h = H$. In summary, the EBSDE (72) admits a solution (74) whose coefficients are determined uniquely from (77)–(80) provided that B and $\bar{\psi}$ are sufficiently small. Notably, the condition (66) is satisfied in this case as W_t is a linear combination of X_t, $Y_t^{(r_i)}$ (Proposition 1) and their expectations on $\mathbb{Q}(\phi)$ are bounded by a positive constant independent from T.

In summary, by Proposition 2, we obtain Proposition 4 on the optimality of the EBSDE.

Proposition 4 *Under the assumption of Proposition* 2, *with* (45), *there are sufficiently small* B *and* $\bar{\psi}$ *independent of* n, *such that the EBSD* (72)–(73) *admits a solution* (W, U, η) *given in* (74) *and* (82). *In this case,* $\phi_t = \tilde{\phi}_t = e^{\psi(r)U_t(r,z)}$ *is the worst-case ambiguity, i.e.,* $\phi_t = \phi_t^*$ *as a maximizer of* (23).

5 Application and implications to the infinite-dimensional case

5.1 Worst-case discharge and relative entropy

Owing to the affine nature of the proposed model, each term of the optimized objective (23) is computable in a closed-form. The explanation below is based on the EBSDE, while the same follows if one uses the HJBE due to their equivalence proven in the previous sections.

Assume that the assumption of Proposition 2 is satisfied. As in (13), we have

$$X^* = \limsup_{T \to +\infty} \frac{1}{T} \mathbb{E}_{\mathbb{Q}(\phi^*)} \left[\int_0^T X_s \, \mathrm{d}s \right] = \frac{\rho}{\rho - \omega} \left(\underline{X} + \int_0^{+\infty} \frac{A M_1^*(r)}{1 - B M_1^*(r)} \frac{1}{r} \pi_n(\mathrm{d}r) \right) \tag{83}$$

with $M_1^* = \int_0^{+\infty} e^{\psi(r)\kappa(r)z} z\nu(\mathrm{d}z)$. Then, we obtain the relative entropy in the worst case as

$$R^* = \bar{\psi} \limsup_{T \to +\infty} \frac{1}{T} \mathbb{A}\left(T, \phi^*\right) = \bar{\psi} \left\{ \limsup_{T \to +\infty} \frac{1}{T} \mathbb{E}_{\mathbb{Q}(\phi^*)} \left[\int_0^T X_s \, \mathrm{d}s \right] - H \right\} \tag{84}$$

using (83) and (36) with the fact that $h = H$. Note the normalization by $\bar{\psi}$ in (84).

5.2 Infinite-dimensional case

The optimality results obtained so far suggest under the limit $n \to +\infty$ we arrive at the integral representation of H as

$$H = \rho a \underline{X} + A \int_0^{+\infty} \frac{1}{\psi(r)} \int_0^{\infty} \left(\exp\left(\psi(r)\kappa(r)z \right) - 1 \right) \nu(\mathrm{d}z) \pi(\mathrm{d}r) \tag{85}$$

if it exists. Guessing this limit is not so difficult and its existence follows if $\psi(r) = \bar{\psi} r$ as $\psi(r)\kappa(r) < \beta$ for $r > 0$ in this case. Indeed, the right-hand side of (85) is finite due to

$$\begin{aligned} &\int_0^{+\infty} \frac{1}{\bar{\psi} r} \int_0^{\infty} \left(\exp\left(\bar{\psi} r u(r) z \right) - 1 \right) \nu(\mathrm{d}z) \pi(\mathrm{d}r) \\ &\quad \le \int_0^{+\infty} \frac{1}{\bar{\psi} r} \int_0^{\infty} \left(\exp(\beta z) - 1 \right) \nu(\mathrm{d}z) \pi(\mathrm{d}r) \\ &\quad = \frac{1}{\bar{\psi}} \cdot \int_0^{+\infty} \frac{1}{r} \pi(\mathrm{d}r) \cdot (-\alpha) \Gamma(-\alpha) \beta^{\alpha} \\ &\quad < +\infty \end{aligned} . \tag{86}$$

Therefore, the integral representation (85) is well-defined. However, reformulating the entire process of the control problem from the dynamics to the optimality equations needs to introduce the theory of stochastic control in an infinite dimension. We will further analyze the topic by focusing on generic affine jump-diffusion processes. The convergence under the limit $n \to +\infty$ is examined numerically below.

5.3 Application

The obtained worst-case ambiguity ϕ^*, worst-case objective H, corresponding long-run discharge X^*, and relative entropy R^* are computed with a real dataset. We apply the moment matching method [38, 42] to the data in the midstream station of Hii River, Japan, where the four-year hourly discharge data of a dam site is available since April 2016 [62].

In the downstream reach of this station, we have been analyzing the discharge dynamics as well as habitat suitability of fishery resources [63], where the water abstraction for the agriculture and the water addition from the bypassing water from an upstream branch of the river exist. Therefore, this study area has been chosen as a potential application site of the proposed model.

We assume the Gamma-type density $\pi(\mathrm{d}r) \sim r^{\alpha_r-1}\exp(-r/\beta_r)\,\mathrm{d}r$ with $\alpha_r > 1$ and $\beta_r > 0$, with which we obtain the sub-exponential autocorrelation $\mathrm{Cor}(s) = (1 + (1 - BM_1)\beta_r s)^{-(\alpha_r-1)}$, $s \geq 0$. We identified the parameter values of the supCBI process as follows using the data from the four water years from June 1, 2016, to May 31, 2020: $\alpha = 0.90$ (-), $\beta = 0.0113$ (s/m^3), $A = 0.0109$ (m$^{3\alpha}$/s$^\alpha$/h), $B = 0.0621$ (m$^{3(\alpha-1)}$/s$^{(\alpha-1)}$/h), $\underline{X} = 1.0$ (m^3/s), $\alpha_r = 2.97$ (-), and $\beta_r = 0.0201$ (1/h). We then verify (2) due to $1 - BM_1 = 0.08$. The identified model reproduces the key statistics (average (m^3/s), standard deviation (m^3/s), skewness (-), kurtosis (-)) as follows; average: 5.131 (data) and 5.096 (model), standard deviation 15.45 (data) and 15.53 (model), skewness 11.85 (data) and 11.20 (model), and kurtosis 195.0 (data) and 199.4 (model). The empirical and modeled statistics agree reasonably well.

The worst-case objective H is numerically computed against different values of the coefficient $\bar{\psi}$, where the ambiguity-aversion coefficient of the form $\psi(r) = \bar{\psi}r$ suggested in the theoretical analysis is employed. We have set $\rho = 0.10$ (1/h), and ω (1/h) is chosen so that the target value $\hat{X}$ becomes 10 (m^3/s) as a demonstrative example.

Figure 2 shows the computed H for both the worst-case overestimation and underestimation with the discrete measure π_n determined by the sequence $\eta_i = \bar{\eta}i/n^\gamma$ ($i = 0, 1, 2, \ldots, n$) with $\bar{\eta} = 0.50$ (1/h) and $\gamma = 0.25$, satisfying the convergence condition of Yoshioka [42]. As shown in Fig. 2, the three curves in each case ($n = 800$ (Blue), 1600 (Magenta), 3200 (Red)) are difficult to distinguish from each other, demonstrating that the computed H are already sufficiently accurate at $n = 800$.

The convergence rate of H with respect to the resolution is n is further discussed quantitatively. Table 1 shows the computed H and its error $\mathrm{Er} = H_{\mathrm{Ref}} - H$ with respect to the

Figure 2 Computed *H* for both the worst-case overestimation (upper-half panel) and underestimation (lower-half panel) with different values of the discretization parameter values $n = 800$ (Blue), 1600 (Magenta), 3200 (Red)

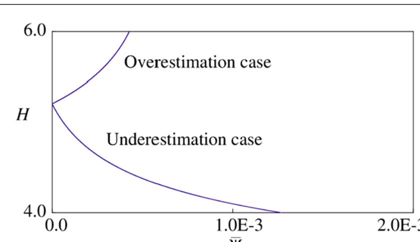

Table 1 Computed H and its error $\mathrm{Er} = H_{\mathrm{Ref}} - H$ with respect to the reference H_{Ref} (H with $n = 6400$) for different values of n. H_{Ref} is 5.8968 (m^3/s) in the overestimation case and is 4.9057 (m^3/s) in the underestimation case. The convergence rate "Conv" at each n is $\log_2(Er|_{n/2}/Er|_n)$

n	Overestimation case			Underestimation case		
	H	Er	Conv	*H*	Er	Conv
3200	5.8966	1.832.E–04	1.49.E+00	4.9056	1.370.E–04	1.49.E+00
1600	5.8963	5.143.E–04	1.11.E+00	4.9053	3.848.E–04	1.11.E+00
800	5.8957	1.108.E–03	9.64.E–01	4.9049	8.287.E–04	9.64.E–01
400	5.8947	2.161.E–03	9.22.E–01	4.9041	1.617.E–03	9.22.E–01
200	5.8927	4.095.E–03		4.9027	3.064.E–03	

reference value H_{Ref} (H with $n = 6400$ as we do not have any analytical solutions) for different values of n for both the overestimation and underestimation cases. The parameter $\bar{\psi}$ of ambiguity-aversion is set as $\bar{\psi} = 0.0004$ (s/m^3), but similar results follow for not too large $\bar{\psi}$ around which H of the overestimation case becomes ill-defined. The table shows that the convergence rate is at a first order with respect to n in both cases, and the errors are sufficiently small with a relatively high resolution. Hereinafter, we use the resolution $n = 3200$ based on this numerical experiment.

Then, we analyze the quantities H, $D^* \equiv X^*/\hat{X}$, and R^* to evaluate the worst-case optimization results. Here, D^* is the ratio between the expected and target discharges, and the deviation between them becomes larger as they deviate from each other. Figs. 3–5 show the computed H, D^*, and R^* as a two-variable function of the target discharge $\hat{X}$ and coefficient $\bar{\psi}$. Each panel (a) in these figures demonstrates that there is a connected region in which the overestimation problem is ill-defined, as expected from the proof of Proposition 2. Each of the quantities H, D^*, and R^* smoothly depends on $\hat{X}$ and $\bar{\psi}$, and the effects of overestimation and underestimation become more negligible as $\bar{\psi}$ gets closer to 0, which is consistent with our intuition. Conversely, the degree of overestimation and underestimation becomes more significant as $\bar{\psi}$ increases with which the worst-case ambiguity ϕ^* exponentially increases and decreases with respect to z, respectively. Note an interesting qualitative difference between the overestimation and underestimation cases

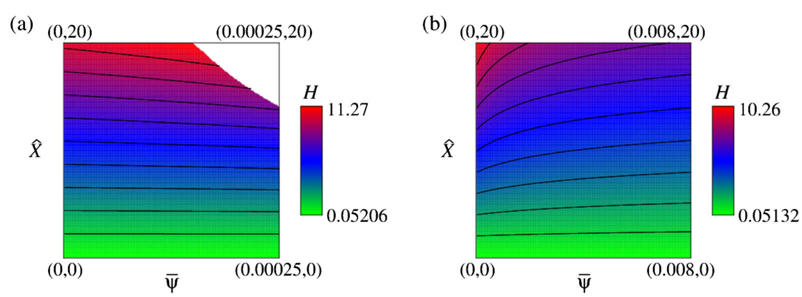

Figure 3 Computed H as a two-variable function of the target discharge $\hat{X}$ and the ambiguity-aversion coefficient $\bar{\psi}$: (a) overestimation case and (b) underestimation case. The contour lines divide the maximum and minimum values into 10 intervals. The white area shows that the problem becomes ill-posed (the positive solution to (37) was not found)

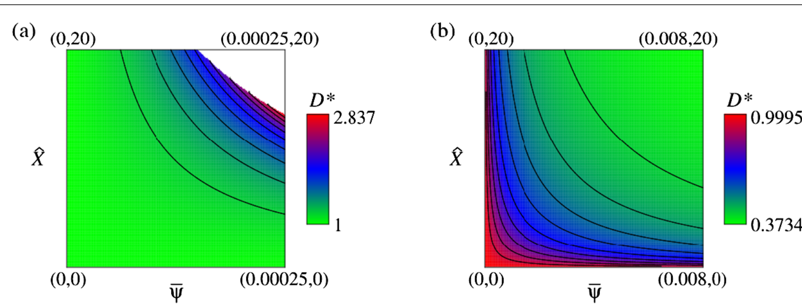

Figure 4 Computed ratio $D^* = X^*/\hat{X}$ as a two-variable function of the target discharge $\hat{X}$ and the ambiguity-aversion coefficient $\bar{\psi}$: (a) overestimation case and (b) underestimation case. The same legends with Fig. 3

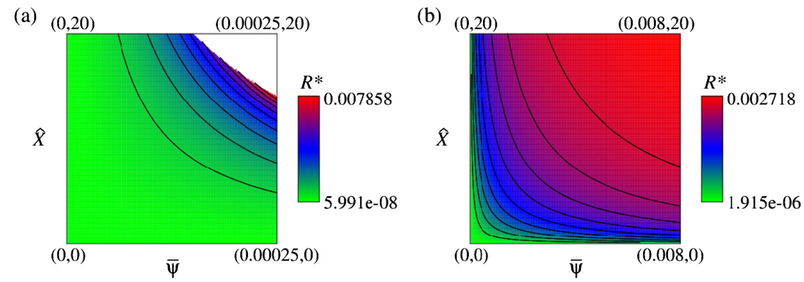

Figure 5 Computed relative entropy R^* as a two-variable function of the target discharge $\hat{X}$ and the ambiguity-aversion coefficient $\bar{\psi}$: (a) overestimation case and (b) underestimation case. The same legends with Fig. 3

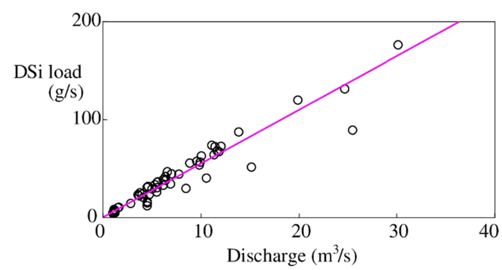

Figure 6 The relationship between the DSi load F (g/s) and discharge X (m^3/s). Circles are measured values and the line is the least-squares fitting ($F = 5.486X + 0.3344$, R^2 value is 0.943)

that the computed quantities change rapidly for large (resp., small) $\hat{X}$, $\bar{\psi}$ in the former (resp., latter).

The computational results suggest that once given the target discharge and ambiguity aversion, both of which will be chosen by an environmental manager, the worst-case discharge X^* and related quantities, such as H and R^*, can be evaluated numerically. Finally, we emphasize that the finite H was obtained due to the parameter-dependent ψ, even for the fine resolution, as theoretically expected from the discussion below Proposition 2. As we demonstrated, one can predict the worst-case discharges and the associated amount of the relative entropy considering the level of ambiguity aversion.

Remark 7 With our framework, we can also evaluate the worst-case optimization problem of an affine functional of the discharge. Indeed, we found an affine relationship between the discharge and DSi load F (g/s) measured in Si. This is a key water quality variable for assessing river environments, particularly for assessing eutrophication. A least-squares fitting with the DSi data (67 sampling data collected from March 26 2019 to December 1 2022) collected at 1.7 km downstream of the discharge station gives the linear relationship between the DSi load F and discharge X as

$$F = f_0 X + f_1 \tag{87}$$

gives $f_0 = 5.486$ (g/m^3) and $f_1 = 0.3344$ (g/s) with the R^2 value 0.943 (Fig. 6). Considering this affine relationship, the worst-case upper and lower bounds of L as a continuous-time scalar stochastic process can be evaluated similarly as the discharge X.

6 Conclusion

We proposed a novel model for the worst-case evaluations of the streamflow discharge under the model ambiguity using the supCBI process. We demonstrated that the optimization results obtained from the HJBE and EBSDE are equivalent to each other. We provided an application example of the proposed model with an existing record of the discharge to show its applicability in a realistic case.

This study thus serves as a case study concerning both optimality equations, simultaneously deepening their understandings. Owing to the affine property of the stochastic process model, a similar methodology can be applied to other affine processes, such as the Hawkes [64] and Volterra processes [65]. The proposed model can also be applied at least formally to nonaffine cases where the HJBE and EBSDE will not be solvable analytically. Some numerical approximation will be necessary in such a case where a Markovian embedding would play a pivotal role, as in this study. Currently, an application of an extended model based on the proposed SDE formulation to a quadratic control problem under incomplete information is under investigation.

Acknowledgements
Japan Society for the Promotion of Science (22K14441), Kurita Water and Environment Foundation (21K008), Environmental Research Projects from the Sumitomo Foundation (203160). A part of this work was conducted during the first author was working at Shimane University, Japan.

Funding
Japan Society for the Promotion of Science (22K14441). Kurita Water and Environment Foundation (21K008). Environmental Research Projects from the Sumitomo Foundation (203160).

Availability of data and materials
Data will be available upon a reasonable request to the corresponding author.

Declarations

Competing interests
The authors declare no competing interests.

Author contributions
HY: Authorization, Formal analysis, Numerical computation, Field survey, Data acquisition, Writing and Editing. *YY:* Field survey, Data acquisition, Writing and Editing. All authors read and approved the final manuscript.

Authors' information
The first author has moved to the new affiliation from Shimane University on April 1 2023.

Author details
[1] Japan Advanced Institute of Science and Technology, 1-1 Asahidai, Nomi, Ishikawa 923-1292, Japan. [2] Shimane University, Nishikawatsu-cho 1060, Matsue 690-8504, Japan.

Received: 9 November 2022 Accepted: 16 June 2023 Published online: 25 July 2023

References

1. Kim SJ, Asadzadeh M, Stadnyk TA. Climate change impact on water supply and hydropower generation potential in Northern Manitoba. J Hydrol Reg Stud. 2022;41:101077. https://doi.org/10.1016/j.ejrh.2022.101077.
2. Wang Y, Tao Y, Qiu R, Wang D, Wu J. A framework for assessing river thermal regime alteration: a case study of the Hanjiang River. J Hydrol. 2022;610:127798. https://doi.org/10.1016/j.jhydrol.2022.127798.
3. White JC, Aspin TWH, Picken JL, Ledger ME, Wilby RL, Wood PJ. Extreme low flow effects on riverine fauna: a perspective on methodological assessments. Ecohydrology. 2022;15(5):e2422. https://doi.org/10.1002/eco.2422.
4. Asselman N, de Jong JS, Kroekenstoel D, Folkertsma S. The importance of peak attenuation for flood risk management, exemplified on the Meuse River, the Netherlands. Water Secur. 2022;15:100114. https://doi.org/10.1016/j.wasec.2022.100114.
5. Zhang C, Ji C, Wang Y, Xiao Q. Flood hydrograph coincidence analysis of the upper Yangtze River and Dongting Lake, China. Nat Hazards. 2022;110(2):1339–60. https://doi.org/10.1007/s11069-021-04993-2.
6. Basso S, Botter G, Merz R, Miniussi A. PHEV! The PHysically-based extreme value distribution of river flows. Environ Res Lett. 2021;16(12):124065. https://doi.org/10.1088/1748-9326/ac3d59.
7. Vázquez-Tarrío D, Menéndez-Duarte R. The estimation of bedload in poorly-gauged mountain rivers. Catena. 2021;204:105425. https://doi.org/10.1016/j.catena.2021.105425.

8. Perri S, Porporato A. Environmental concentrations as ratios of random variables. Environ Res Lett. 2022;17(2):024011. https://doi.org/10.1088/1748-9326/ac4a9f.
9. Yoshioka H, Yoshioka Y. Designing cost-efficient inspection schemes for stochastic streamflow environment using an effective Hamiltonian approach. Optim Eng. 2022;23:1375–407. https://doi.org/10.1007/s11081-021-09655-7.
10. Song X, Zhong D, Wang G. A study of the stochastic evolution of hydraulic geometry relationships. River Res Appl. 2019;35(7):867–80. https://doi.org/10.1002/rra.3461.
11. Durighetto N, Mariotto V, Zanetti F, McGuire KJ, Mendicino G, Senatore A, Botter G. Probabilistic description of streamflow and active length regimes in rivers. Water Resour Res. 2022;58(4):e2021WR031344. https://doi.org/10.1029/2021WR031344.
12. Yoshioka H, Yoshioka Y. A simple model on streamflow management with a dynamic risk measure. In: Proceedings of the seventh international conference on mathematics and computing. Singapore: Springer; 2022. p. 943–51. https://doi.org/10.1007/978-981-16-6890-6_71.
13. Caponi F, Vetsch DF, Siviglia A. A model study of the combined effect of above and below ground plant traits on the ecomorphodynamics of gravel bars. Sci Rep. 2020;10(1):1–14. https://doi.org/10.1038/s41598-020-74106-9.
14. Øksendal B, Sulem A. Applied stochastic control of jump diffusions. Cham: Springer; 2019.
15. Delong Ł. Backward stochastic differential equations with jumps and their actuarial and financial applications. London: Springer; 2013.
16. Fleming WH, Soner HM. Controlled Markov processes and viscosity solutions. New York: Springer; 2006.
17. Christara CC, Wu R. Penalty and penalty-like methods for nonlinear HJB PDEs. Appl Math Comput. 2022;425:127015. https://doi.org/10.1016/j.amc.2022.127015.
18. Dleuna Nyoumbi C, Tambue A. A novel high dimensional fitted scheme for stochastic optimal control problems. Comput Econ. 2023;61:1–34. https://doi.org/10.1007/s10614-021-10197-4.
19. Hubert E, Mastrolia T, Possamaï D, Warin X. Incentives, lockdown, and testing: from Thucydides' analysis to the COVID-19 pandemic. J Math Biol. 2022;84:37. https://doi.org/10.1007/s00285-022-01736-0.
20. Li Y, Zheng H. Dynamic convex duality in constrained utility maximization. Stochastics. 2018;90(8):1145–69. https://doi.org/10.1080/17442508.2018.1480023.
21. Molla HU, Qiu J. Numerical approximations of coupled forward–backward SPDEs. Stoch Anal Appl. 2021;41(2):291–326. https://doi.org/10.1080/07362994.2021.2011318.
22. Mu X, Zhang Q. Optimal strategy of vaccination and treatment in an SIRS model with Markovian switching. Math Methods Appl Sci. 2019;42(3):767–89. https://doi.org/10.1002/mma.5378.
23. Yoshioka H. Towards control of dam and reservoir systems with forward-backward stochastic differential equations driven by clustered jumps. Adv Control Appl. 2022;4(2):e104. https://doi.org/10.1002/adc2.104.
24. Xiao L, Fan S, Tian D. Probabilistic interpretation of HJB equations by the representation theorem for generators of BSDEs. Electron Commun Probab. 2020;25:1–10. https://doi.org/10.1214/20-ECP310.
25. Wu X, Marshall L, Sharma A. Incorporating multiple observational uncertainties in water quality model calibration. Hydrol Process. 2022;36(1):e14452. https://doi.org/10.1002/hyp.14452.
26. Potash E, Steinschneider S. A Bayesian approach to recreational water quality model validation and comparison in the presence of measurement error. Water Resour Res. 2022;58:e2021WR031115. https://doi.org/10.1029/2021WR031115.
27. Anderson EW, Hansen LP, Sargent TJ. A quartet of semigroups for model specification, robustness, prices of risk, and model detection. J Eur Econ Assoc. 2003;1(1):68–123.
28. Rubtsov A, Xu W, Šević A, Šević Ž. Price of climate risk hedging under uncertainty. Technol Forecast Soc Change. 2021;165:120430. https://doi.org/10.1016/j.techfore.2020.120430.
29. Hansen LP, Miao J. Asset pricing under smooth ambiguity in continuous time. 2022. University of Chicago, Becker Friedman Institute for Economics Working Paper, (2022-39).
30. Petracou EV, Xepapadeas A, Yannacopoulos AN. Decision making under model uncertainty: Fréchet–Wasserstein mean preferences. Manag Sci. 2022;68(2):1195–211. https://doi.org/10.1287/mnsc.2021.3961.
31. Agliardi E, Xepapadeas A. Temperature targets, deep uncertainty and extreme events in the design of optimal climate policy. J Econ Dyn Control. 2022;139:104425. https://doi.org/10.1016/j.jedc.2022.104425.
32. Yoshioka H, Tsujimura M, Hamagami K, Yoshioka Y. A simple stochastic process model for river environmental assessment under uncertainty. In: International conference on computational science. Cham: Springer; 2020. p. 494–507. https://doi.org/10.1007/978-3-030-50436-6_36.
33. Yoshioka H, Tsujimura M. Hamilton–Jacobi–Bellman–Isaacs equation for rational inattention in the long-run management of river environments under uncertainty. Comput Math Appl. 2022;112:23–54. https://doi.org/10.1016/j.camwa.2022.02.013.
34. Øksendal B, Sulem A. Forward–backward stochastic differential games and stochastic control under model uncertainty. J Optim Theory Appl. 2014;161(1):22–55. https://doi.org/10.1007/s10957-012-0166-7.
35. Horst U, Xia X, Zhou C. Portfolio liquidation under factor uncertainty. Ann Appl Probab. 2022;32(1):80–123. https://doi.org/10.1214/21-AAP1672.
36. Casgrain P, Jaimungal S. Mean-field games with differing beliefs for algorithmic trading. Math Finance. 2020;30(3):995–1034. https://doi.org/10.1111/mafi.12237.
37. Firoozi D, Jaimungal S. Exploratory LQG mean field games with entropy regularization. Automatica. 2022;139:110177. https://doi.org/10.1016/j.automatica.2022.110177.
38. Yoshioka H. Fitting a superposition of Ornstein-Uhlenbeck processes to time series of discharge in a perennial river environment. ANZIAM J. 2022;63:C84–96. https://doi.org/10.21914/anziamj.v63.16985.
39. Yoshioka H, Tsujimura M, Tanaka T, Yoshioka Y, Hashiguchi A. Modeling and computation of an integral operator Riccati equation for an infinite-dimensional stochastic differential equation governing streamflow discharge. Comput Math Appl. 2022;2022(126):115–48. https://doi.org/10.1016/j.camwa.2022.09.009.
40. Ledvinka O, Recknagel T. Long-term persistence in discharge time series of mountainous catchments in the Elbe River basin. Proc Int Assoc Hydrol Sci. 2020;383:135–40. https://doi.org/10.5194/piahs-383-135-2020.
41. Wu W, Yuan N, Xie F, Qi Y. Understanding long-term persistence and multifractal behaviors in river runoff: a detailed study over eastern China. Physica A. 2019;533:122042. https://doi.org/10.1016/j.physa.2019.122042.

42. Yoshioka H. A supCBI process with application to streamflow discharge and a model reduction. 2022. preprint. https://arxiv.org/abs/2206.05923.
43. Yoshioka H, Tanaka T, Yoshioka Y, Hashiguchi A. Stochastic optimization of a mixed moving average process for controlling non-Markovian streamflow environments. Appl Math Model. 2023;116:490–509. https://doi.org/10.1016/j.apm.2022.11.009.
44. Grahovac D, Leonenko NN, Sikorskii A, Taqqu MS. The unusual properties of aggregated superpositions of Ornstein–Uhlenbeck type processes. Bernoulli. 2019;25(3):2029–50. https://doi.org/10.1214/18-EJS1523.
45. Cuchiero C, Teichmann J. Markovian lifts of positive semidefinite affine Volterra-type processes. Decis Econ Finance. 2019;42(2):407–48. https://doi.org/10.1007/s10203-019-00268-5.
46. Baltas I, Xepapadeas A, Yannacopoulos AN. Robust control of parabolic stochastic partial differential equations under model uncertainty. Eur J Control. 2019;46:1–13. https://doi.org/10.1016/j.ejcon.2018.04.004.
47. Cohen SN, Fedyashov V. Ergodic BSDEs with jumps and time dependence. 2014. preprint. https://arxiv.org/abs/1406.4329.
48. Guambe C, Mabitsela L, An KR. Ergodic BSDE risk representation in a jump-diffusion framework. Int J Theor Appl Finance. 2021;24(03):2150015. https://doi.org/10.1142/S0219024921500151.
49. Arapostathis A, Caffarelli L, Pang G, Zheng Y. Ergodic control of a class of jump diffusions with finite Lévy measures and rough kernels. SIAM J Control Optim. 2019;57(2):1516–40. https://doi.org/10.1137/18M1166717.
50. Fuhrman M, Hu Y, Tessitore G. Ergodic BSDEs and optimal ergodic control in Banach spaces. SIAM J Control Optim. 2019;48(3):1542–66. https://doi.org/10.1137/07069849X.
51. Chong WF, Hu Y, Liang G, Zariphopoulou T. An ergodic BSDE approach to forward entropic risk measures: representation and large-maturity behavior. Finance Stoch. 2019;23(1):239–73. https://doi.org/10.1007/s00780-018-0377-3.
52. Sun Z, Zhang X, Li YN. A BSDE approach for bond pricing under interest rate models with self-exciting jumps. Commun Stat, Theory Methods. 2021;50(14):3249–61. https://doi.org/10.1080/03610926.2019.1691234.
53. Pasricha P, Selvamuthu D, Tardelli P. Hedging and utility valuation of a defaultable claim driven by Hawkes processes. Appl Stoch Models Bus Ind. 2022;38(2):334–52. https://doi.org/10.1002/asmb.2663.
54. Syvitski J, Ángel JR, Saito Y, Overeem I, Vörösmarty CJ, Wang H, Olago D. Earth's sediment cycle during the Anthropocene. Nat Rev Earth Environ. 2022;3:179–96. https://doi.org/10.1038/s43017-021-00253-w.
55. Chifflard P, Zepp H. Investigation of subsurface connectivity and subsurface stormflow in low mountain ranges—findings from the two research catchments Obere Brachtpe and Bohlmicke (Germany). Hydrol Process. 2022;36(2):e14505. https://doi.org/10.1002/hyp.14505.
56. Nakajima T, Sugimoto R, Kusunoki T, Yokoyama K, Taniguchi M. Nutrient fluxes from rivers, groundwater, and the ocean into the coastal embayment along the Sanriku ria coast, Japan. Limnol Oceanogr. 2021;66(7):2728–44. https://doi.org/10.1002/lno.11785.
57. Li Z. Measure-valued branching Markov processes. Berlin: Springer; 2011.
58. Fallahgoul H, Loeper G. Modelling tail risk with tempered stable distributions: an overview. Ann Oper Res. 2021;299(1):1253–80. https://doi.org/10.1007/s10479-019-03204-3.
59. Barndorff-Nielsen OE, Stelzer R. Multivariate supOU processes. Ann Appl Probab. 2011;21(1):140–82. https://doi.org/10.1214/10-AAP690.
60. Stelzer R, Tosstorff T, Wittlinger M. Moment based estimation of supOU processes and a related stochastic volatility model. Stat Risk Model. 2015;32(1):1–24. https://doi.org/10.1515/strm-2012-1152.
61. Hess M. Optimal equivalent probability measures under enlarged filtrations. J Optim Theory Appl. 2019;183(3):813–39. https://doi.org/10.1007/s10957-019-01581-0.
62. Ministry of Land, Infrastructure, Transport and Tourism (MLIT). 2022. http://www1.river.go.jp/cgi-bin/SrchDamData.exe?ID=607041287705020&KIND=1&PAGE=0. Last accessed on May 25.
63. Tanaka T, Yoshioka H, Yoshioka Y. DEM-based river cross-section extraction and 1-D streamflow simulation for eco-hydrological modeling: a case study in upstream Hiikawa River, Japan. Hydrol Res Lett. 2021;15(3):71–6. https://doi.org/10.3178/hrl.15.71.
64. Kramer A, Kiesel R. Exogenous factors for order arrivals on the intraday electricity market. Energy Econ. 2021;97:105186. https://doi.org/10.1016/j.eneco.2021.105186.
65. Dupret JL, Hainaut D. Portfolio insurance under rough volatility and Volterra processes. Int J Theor Appl Finance. 2021;24(06n07):2150036. https://doi.org/10.1142/S0219024921500369.

Publisher's Note